NATIONAL ADVISORY COMMITTEE FOR AERONAUTICS

REPORT No. 374

THE AUTOMOTIVE IGNITION COIL

By T. H. DARNELL

1931

For sale by the Superintendent of Documents, Washington, D. C. - - - - - - - - - Price 25 cents

AERONAUTICAL SYMBOLS

1. FUNDAMENTAL AND DERIVED UNITS

	Symbol	Metric		English	
		Unit	Symbol	Unit	Symbol
Length	l	meter	m	foot (or mile)	ft. (or mi.)
Time	t	second	s	second (or hour)	sec. (or hr.)
Force	F	weight of one kilogram	kg	weight of one pound	lb.
Power	P	kg/m/s		horsepower	hp
Speed		km/hr	k. p. h.	mi./hr.	m. p. h.
		m/s	m. p. s.	ft./sec.	f. p. s.

2. GENERAL SYMBOLS, ETC.

W, Weight, $=mg$

g, Standard acceleration of gravity $=9.80665$ m/s^2 $=32.1740$ ft./sec.^{2}

m, Mass, $=\frac{W}{g}$

ρ, Density (mass per unit volume).

Standard density of dry air, 0.12497 (kg-m^{-4} s^2) at 15° C and 760 mm $=0.002378$ (lb.-ft.$^{-4}$ sec.^{2}).

Specific weight of "standard" air, 1.2255 kg/m^3 $=0.07651$ lb./ft.^{3}

mk^2, Moment of inertia (indicate axis of the radius of gyration, k, by proper subscript).

S, Area.

S_w, Wing area, etc.

G, Gap.

b, Span.

c, Chord length.

b/c, Aspect ratio.

f, Distance from C. G. to elevator hinge.

μ, Coefficient of viscosity.

3. AERODYNAMICAL SYMBOLS

V, True air speed.

q, Dynamic (or impact) pressure $=\frac{1}{2}\rho V^2$

L, Lift, absolute coefficient $C_L=\frac{L}{qS}$

D, Drag, absolute coefficient $C_D=\frac{D}{qS}$

C, Cross-wind force, absolute coefficient $C_C=\frac{C}{qS}$

R, Resultant force. (Note that these coefficients are twice as large as the old coefficients L_C, D_C.)

i_w, Angle of setting of wings (relative to thrust line).

i_t, Angle of stabilizer setting with reference to thrust line.

γ, Dihedral angle.

$\rho\frac{Vl}{\mu}$, Reynolds Number, where l is a linear dimension.

e. g., for a model airfoil 3 in. chord, 100 mi./hr. normal pressure, 0° C: 255,000 and at 15° C., 230,000;

or for a model of 10 cm chord 40 m/s, corresponding numbers are 299,000 and 270,000.

C_p, Center of pressure coefficient (ratio of distance of C. P. from leading edge to chord length).

β, Angle of stabilizer setting with reference to lower wing, $=(i_t-i_w)$.

α, Angle of attack.

ϵ, Angle of downwash.

REPORT No. 374

THE AUTOMOTIVE IGNITION COIL

By T. H. DARNELL
Bureau of Standards

27715—31——1

NATIONAL ADVISORY COMMITTEE FOR AERONAUTICS

NAVY BUILDING, WASHINGTON, D. C.

(An independent Government establishment, created by act of Congress approved March 3, 1915, for the supervision and direction of the scientific study of the problems of flight. Its membership was increased to 15 by act approved March 2, 1929 (Public, No. 908, 70th Congress). It consists of members who are appointed by the President, all of whom serve as such without compensation.)

EXECUTIVE COMMITTEE

REPORT No. 374

THE AUTOMOTIVE IGNITION COIL[1]

By T. H. Darnell

SUMMARY

This paper which was submitted by the Bureau of Standards for publication gives the results of an extensive series of measurements on the secondary voltage induced in an ignition coil of typical construction under a variety of operating conditions. These results show that the theoretical predictions hitherto made as to the behavior of this type of apparatus are in satisfactory agreement with the observed facts. The large mass of data obtained is here published both for the use of other investigators who may wish to compare them with other theoretical predictions and for the use of automotive engineers who will here find definite experimental results showing the effect of secondary capacity and resistance on the crest voltage produced by ignition apparatus.

INTRODUCTION

The induction coil is in wide use throughout the world as the source of high potential necessary for the ignition of explosive charges in gas engines. When used for this purpose it is called an ignition coil, and in one form or another is to be found as an integral part of all internal combustion engines other than those of the Diesel type. Its importance as commercial apparatus is thus clearly manifest.

Although simple in appearance and construction, the induction coil operates in a complicated manner. The theory of its operation has been extensively treated mathematically by many investigators, but until the present work only meager experimental checks on the theory were available. This because of the nonexistence of suitable apparatus.

The induction coil consists of two coils, one usually surrounding the other, wound upon an iron core. One winding, called the primary, is composed of a few turns of coarse wire. The other winding, the secondary, is made up of a large number of turns of fine wire. The two windings may or may not be connected. When an electric current through the primary is suddenly interrupted, a high potential is induced between the terminals of the secondary. The main problem is the nature of this potential.

Mathematical theory (Reference 1) shows that the secondary potential is oscillatory, and moreover that the wave is composed of two superimposed frequencies, the higher of which generally is not a harmonic of the lower, nor do their crests occur simultaneously. The maximum voltage attained by the wave is easily measured by means of a calibrated sphere gap, but the frequencies and potentials involved are of too high an order to be satisfactorily handled by the ordinary oscillograph. The problem of obtaining the actual wave shape is thus seen to be rather difficult, nevertheless two independent investigators have attacked it with some success.

E. Taylor-Jones (Reference 2) devised a special electrostatic oscillograph with which he successfully photographed the wave. The presence of the two frequencies was clearly shown as predicted, but the oscillograms failed to record the true wave shape in that the deflection of the oscillograph was proportional to the square of the voltage. N. R. Campbell (Reference 3), by using an elaborate point-by-point method, obtained a sufficient number of values to plot the wave. Remarkable as was this achievement, its results applied only to a special case.

The cathode ray oscillograph is an instrument capable of handling frequencies of the order of 10^6 at high potentials. The recent development of auxiliary switching apparatus further extends its usefulness into the field of nonrecurrent phenomena. With this apparatus it is thus an easy matter to photograph in its natural form and with a high degree of accuracy the secondary voltage wave of an induction coil. Through fortunate circumstances equipment of the necessary nature was for a period available to the author. The results are shown below.

OUTLINE OF INVESTIGATION

In order to enhance the practical value of the work it was decided to use standard automobile ignition coils, as it seemed better to study two coils intensively, rather than to obtain a few data about several. Accordingly a coil and a distributor were borrowed from each of two representative manufacturers.

In the external circuits of the ignition coil there are four constants which are easily variable and which are

[1] With a note by F. B. Silsbee, Bureau of Standards.

Publication has been approved by the Massachustts Institute of Technology, where the paper was accepted as a thesis (M. S.), and by the General Electric Co., in whose laboratories much of the work was done.

of paramount importance. These are the voltage applied to the primary winding, the capacity shunted across the breaker which interrupts the primary current, the capacity shunted across the secondary, and the resistance shunted across the secondary. The main plan of the investigation was to take series of oscillograms during which one of these factors was varied through as wide a range as feasible while the others were held constant. To interconnect the series a standard value was set for each circuit quantity which was always held at the standard value unless it itself was being varied. These standards were as follows: For the primary voltage, a 6-volt storage battery; for the breaker capacity, the condenser ($0.22\mu f$) furnished by the manufacturer with the breaker; for the shunted secondary capacity, only that of the oscillograph ($23\mu\mu f$ and lead wires); and for the secondary shunted resistance, likewise only that of the oscillograph, 11 megohms.

In addition to the series mentioned above, a series of oscillograms was taken with varying primary voltage, during which an external inductance was included in the primary circuit, concerning which more is said later. Additional records of various sorts such as those of the current in the primary circuit, the voltage across the primary, etc., were also taken.

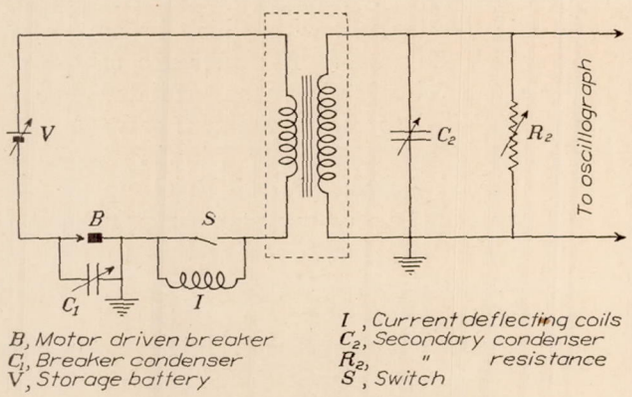

FIGURE 1.—Connections used in measurements

SET-UP AND APPARATUS

A modified Dufour cathode ray oscillograph was used to take the oscillograms. Since it has been completely treated elsewhere (Reference 4) only a brief description of its operation is given here. In this oscillograph the film is mounted in the vacuum chamber, allowing high speed recording by a single exposure. A cold cathode tube is used, the cathode voltage being applied for an interval of time only slightly longer than that necessary for recording. The cathode beam passes down between a pair of deflecting plates, between two sets of deflecting coils, and then directly on to the film. The two sets of deflecting coils are mounted in the same plane with their axes at right angles to each other and to the path of the beam. A suitable transient current, called the sweeping current, applied to one set of deflecting coils moves the cathode beam across the film, producing the time axis. The other set of deflecting coils is used either for recording transient currents or the undamped high frequency current from an external oscillator, which serves as a convenient calibration of the time axis. The transient voltage to be photographed is applied to the deflecting plates, either directly or through a resistance voltage divider. The resistance of the divider is so large and the capacity of the deflecting plates so small that no appreciable energy is drawn from the transient circuit. Within the limits of the film dimensions, the voltage deflection is practically linear.

The timing of the cathode voltage and the sweeping current so that they are applied to the oscillograph during the same interval of time is automatically done by a synchronous switch. The switch can be made to perform an additional service by connecting an auxiliary circuit to it before the taking of an oscillogram. When this is done the switch applies the cathode voltage and the sweeping current to the oscillograph as usual for the taking of the picture, but immediately after the recording disconnects the deflecting plates from the transient circuit and connects them to a source of constant known voltage, and further applies the cathode voltage and the sweeping current to the oscillograph, thus causing a second exposure to be made, but this time with a constant voltage on the deflecting plates. This second exposure produces a straight line of uniform deflection, and since the voltage causing the deflection is known, serves as a calibration of the film.

The general connections of the set-up are shown in Figure 1. The current deflecting coils of the oscillograph were included in the primary circuit only when it was desired to record the primary current. The breaker B was the breaker mechanism of a standard Delco automobile distributor less its condenser. The condensers used across the breaker at C_1 were paraffin paper condensers, those across the secondary at C_2 mica or air condensers. The resistors used across the secondary at R_2 were water tubes. The ignition coils tested were a standard Delco and a standard Northeast, such as are ordinarily used with automobile engines.

The breaker was rigidly connected to and driven by the rotor of a 1,200-revolution per minute synchronous motor. The stator of this motor was not fixed in position, but could be rotated several degrees in either direction around its axis by means of a screw adjustment. Once properly adjusted, the stator could be clamped in position. The object of this stator adjustment was to provide a means of shifting the times at which the breaker interrupted the primary current until the formation of the secondary voltage wave coincided with the application of cathode voltage and sweeping current to the oscillograph. Such is the only condition under which the desired oscillogram will be obtained.

Connections in the primary circuit were made with twisted pair lamp cord. The ignition coil under observation was placed as close as possible to the oscillograph, so that the high potential secondary connection was straight and never more than 8 inches in length.

EXPERIMENTAL PROCEDURE

Operation of the apparatus was comparatively simple. Adjustments were greatly facilitated through the use of an observation window in the side of the oscillograph and a fluorescent screen which could be moved up to cover the films and protect them from exposure during adjustments. Being subject to direct impact of the cathode beam, the screen would fluoresce brilliantly enough and for a sufficient length of time to give an observer looking through the window a clear impression of the transient occurring while the beam was moving across the screen.

Thus by adjusting the position of the stator of the breaker-driving motor and observing the resultant change in position of the secondary voltage wave on the screen, that portion of the wave which it was desired to photograph was easily brought into the field of action. The portion of the wave appearing on the oscillogram was changed by adjusting the sweeping current, which controlled the speed of the beam in moving across the plate and thus determined the time scale of the film.

In taking a picture the procedure was as follows: The external circuits of the ignition coil were adjusted to the values for which an oscillogram was desired. The breaker-driving motor was started, voltage was applied to the primary circuit, and any adjustments necessary to bring the desired portion and amount of the wave onto the film were made. When everything appeared satisfactory, the observation window was covered, the fluorescent screen lowered so as to uncover the film, and the synchronous switch connected to produce automatic voltage calibration. A single push on the operating button then caused two exposures, the desired voltage wave, and a voltage calibration line. As soon as these exposures had been made, as shown by successive flashes of the cathode tube, the voltage was removed from the primary circuit and power applied to the high-frequency oscillator which was already connected to the second set of deflecting coils. The operating button was pushed for the second time, causing the third exposure, that of the high-frequency current used for time calibration. The third exposure made, power was removed from the oscillator and the fourth exposure taken without voltage on the deflecting plates or current in the deflecting coils. The resultant straight line, having neither voltage nor current deflection, is a zero reference axis. After the fourth exposure, the screen was again raised to cover the films, the observation window uncovered, and the whole process repeated for the following oscillogram.

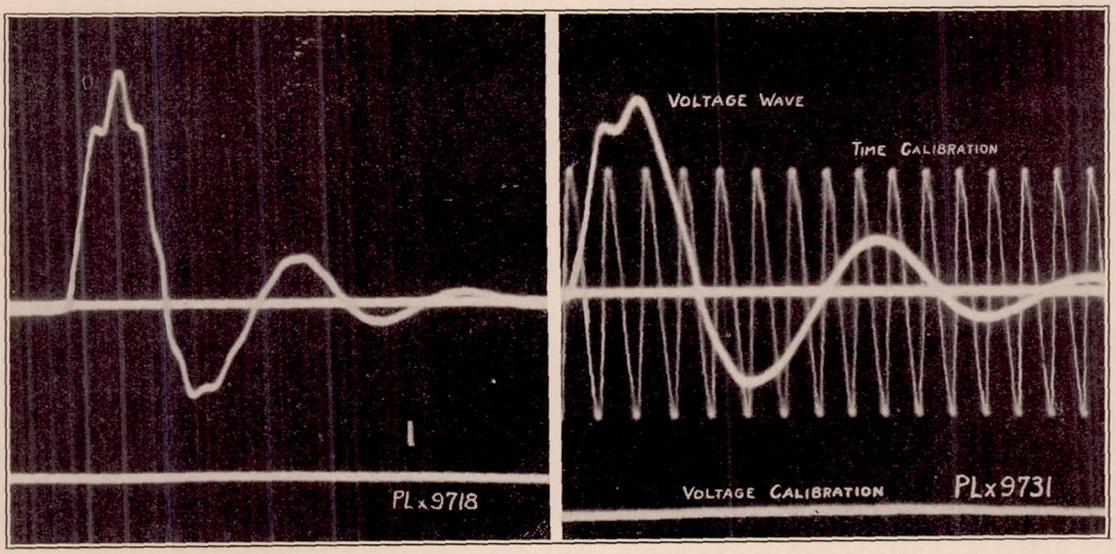

FIGURE 2.—Secondary voltage waves versus time under normal conditions, northeast (PL×9718) and Delco (PL×9731)

GENERAL DISCUSSION OF RESULTS

Some 450 oscillograms were taken, of which more than 350 were directly measured and used in determining the results given below. A typical oscillogram of the secondary voltage wave of each coil is shown in Figure 2. These prints were made from films taken under what is referred to as the "normal" condition; i. e., the condition where all circuit quantities were adjusted to their standard values. Film PL×9731 contains four separate exposures, viz., the straight horizontal line across the center of the film, which is the zero reference axis; the regular undamped oscillation across the center of the film, which is a 15-kilocycle timing wave; the straight horizontal line across the bottom of the film, which is the voltage calibration line; and, the irregular damped oscillation, which is the desired secondary voltage wave. Film PL×9718 lacks the timing wave but contains the other three exposures of PL×9731.

An inspection of the secondary voltage wave indicates that in general it is composed of two oscillating components; one of relatively small amplitude and high frequency, the other of relatively large amplitude and low frequency. Having obtained the wave, there thus remains the problem of analyzing it; i. e., separating the components and finding the amplitudes and frequencies of each. Throughout the remainder of this report the component of large amplitude is referred to as the "principal" component; the one of small amplitude, as the "secondary" component. The actual secondary voltage wave is spoken of as the "main" wave.

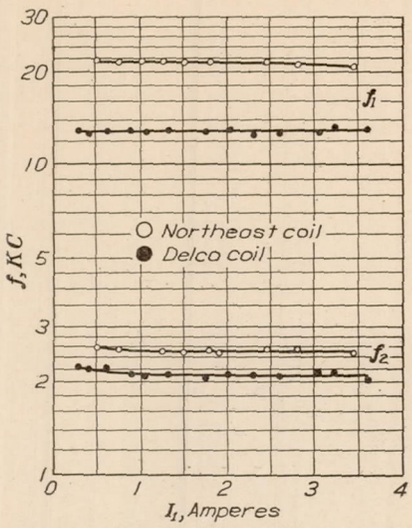

FIGURE 3.—Frequency of oscillations versus primary current at break. f_1 is frequency of secondary component, i. e., that having smaller amplitude. f_2 is frequency of principal component, i. e., that having larger amplitude.

The instant at which the breaker interrupts the current in the primary circuit is always represented on the main wave oscillogram by the point at which the voltage of the main wave begins to rise.

Methods of determining voltages and frequencies are described in the appendix. The methods employed to determine the frequencies of the components, while only approximate, gave very satisfactory results. A frequency analysis was made of practically every film, the results of which probably constitute the major quantitative part of the investigation.

The component voltages, however, proved to be more difficult. Various methods of analysis, all involving considerable approximations, were suggested, but none gave any particular degree of success.

Another quantity, the maximum voltage attained by any half cycle of the main wave, is of importance, and fortunately was easily obtainable. Although open to question as used, this maximum was evaluated in practically all cases for every half cycle, up to and including the fourth, appearing on the film.

Both good and bad oscillograms were obtained. Considerable trouble was encountered from intermittent electron emission of the cathode tube, which resulted in breaks or gaps in the recording. Such breaks are particularly evident in the voltage calibration lines. Some trouble was also had with faulty operation of the synchronous switch, which might give spurious results. In all cases, however, the poor quality of any film must be charged to the operator, rather than to the apparatus.

SERIES WITH VARYING PRIMARY VOLTAGE

As mentioned in the introduction, these series of oscillograms were obtained with all of the circuit constants except the primary voltage maintained at their standard values. As the primary voltage is of no importance except as it affects the current existing in the primary at the instant the breaker opens the primary circuit, no attempt was made to record with any accuracy the varying primary voltages used. Instead, separate oscillograms of the primary current were taken by means of a regular Duddell oscillograph. This oscillograph, while not fast enough to record the oscillations of the current after the break with any accuracy, was capable of accurately measuring the current at the instant of the break, which is the desired quantity. Energy to operate this oscillograph was furnished by a 0.1 ohm shunt inserted into the primary circuit. The timing of the Duddell oscillograph, so that it photographed the current at the particular interruption for which the secondary voltage wave was photographed on the Dufour oscillograph, was controlled by the synchronous switch.

No appreciable change in wave shape with varying currents in the primary at break was observed for either coil, all oscillograms having the same appearance as those shown in Figure 2. This indicates that both coils were operated well below the saturation point.

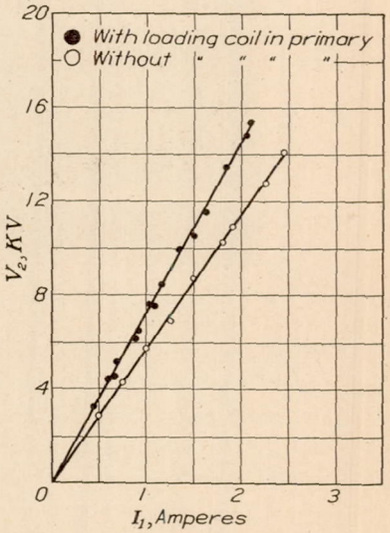

FIGURE 4.—Secondary crest voltage versus primary current at break, for Northeast coil

Curves of the measured frequencies of the two components are shown in Figure 3. In this graph, as well as subsequent ones, f_2 is the frequency of the principal component, and f_1 that of the secondary component. As is to be expected, the frequency of each component is practically constant. The slight rise in frequency of the principal components at the low end of the scale is probably due to a nonlinear current-magnetization relationship.

Curves of the observed maximum secondary voltage plotted against primary current at break are shown in Figure 4 for the Northeast coil, and in Figure 5 for the Delco coil. The straight line through the open circles confirms the familiar relationship predicted and checked by previous investigators (Reference 5).

The line through the solid circles represents an additional series which is of interest. During this series an external inductance was connected in series in the primary circuit. This inductance was that of the current deflecting coils of the Dufour oscillograph. The oscillograms taken in the series were not the usual secondary voltage-time pictures, but secondary voltage-primary current pictures. In taking such oscillograms no sweeping current was employed, the primary current causing deflections of the beam in the direction at right angles to the secondary voltage deflections. Examples of such oscillograms are shown in Figures 23 and 24, and are discussed in a later section. It is sufficient here to simply say that such an oscillogram gives both the value of the primary current at break and the maximum secondary voltage with a single recording.

It is interesting to note that the curve for operation with an external inductance is steeper than the one for normal operation. This curious fact, that for a given primary current at break a greater secondary voltage is produced when there is an external inductance in the primary circuit, was predicted and checked in a few instances by E. Taylor-Jones (Reference 6).

SERIES WITH VARYING BREAKER CAPACITY

Northeast coil.—Very great changes in the shape of the secondary voltage wave were observed with varying breaker capacities. Oscillograms for some 40 different values of this capacity were taken. Twelve such, selected so as to show the major changes in wave shape, are shown in Figure 6. In each case the value of the breaker capacity used is marked at the bottom of the oscillogram. The order of arrangement in the figure in the direction of increasing capacity is from left to right in the top row, from right to left in the middle row, and from left to right in the bottom row; or, roughly the shape of a reversed letter S. The capacity used for the first film, PL9745, was the minimum obtainable, namely that of the breaker mechanism itself and the leads to it. Subsequent measurement indicates that it is of the order of 500 micromicrofarads.

In comparing the oscillograms in any series it should be borne in mind that the deflection for a given voltage or a given interval of time varies from film to film on account of the uncontrolled as well as controlled factors. The principal source of uncontrolled variation was the internal vacuum of the oscillograph, which was often appreciably different for different oscillograms. As the cathode beam was sensitive to changes in this vacuum, the result was small, but appreciable variations in the standard deflections for different films. Thus the maximum voltage for the first half cycle is approximately the same in each of the first three oscillograms of Figure 6, although the deflection for the maximum voltage is noticeably greatest in the third, PL9755.

The standard deflections could be, and naturally were, varied through a wide range by changing the external adjustments of the oscillograph. Thus the sweeping speed in the first oscillogram of Figure 6, PL9745, is approximately twice as fast as in the other films shown in the figure.

With these reservations in mind several interesting facts are apparent from an observation of Figure 6. The amplitude of the secondary component is very small for low values of the breaker capacity, but up to a certain point increases as this capacity increases. Beyond this point the amplitude decreases, until, when very large values of breaker capacity are used,

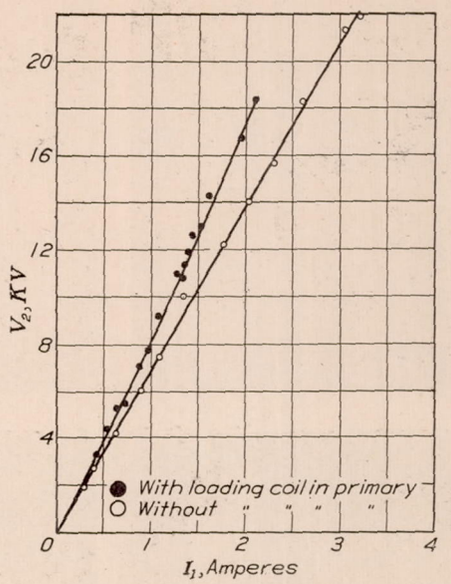

FIGURE 5.—Secondary crest voltage versus primary current at break, for Delco coil

it is again quite small. On the other hand the amplitude of the principal component steadily decreases with an increase of breaker capacity.

The frequency of the principal component decreases continuously with an increase of capacity. Likewise that of the secondary component, which up to a certain point decreases faster than does that of the principal component, as is shown by the fact that up to this point the secondary component humps on the main wave move clockwise around it. Beyond this point, which occurs approximately at film PL9777, the secondary component humps move counterclockwise around the main wave, indicating that the frequency of the secondary component is changing at a rate slower than that of the principal component.

These last conclusions are also evident from Figure 7, which contains curves of the component frequencies. The continuous curves are drawn as nearly as possible through those represented by the observed values.

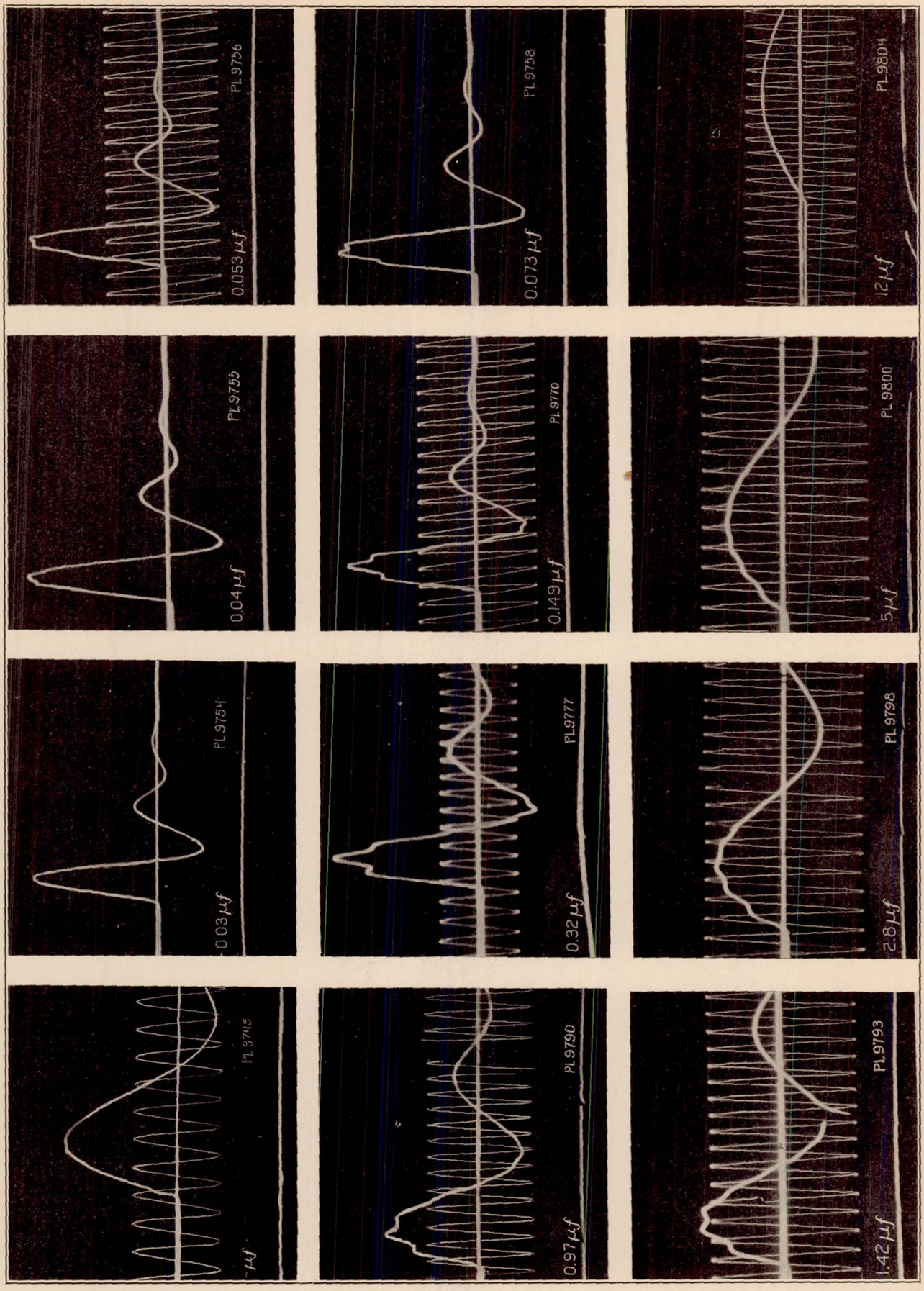

FIGURE 6.—Secondary voltage versus time for various values of primary capacity, Northeast coil

The dotted curves are those for the frequencies of the two components given by the theoretical equation (7):

$$8\pi^2 f^2 = \left(\frac{1}{L_1C_1} + \frac{1}{L_2C_2}\right) \pm \sqrt{\left(\frac{1}{L_1C_1} + \frac{1}{L_2C_2}\right)^2 - \frac{4(1-k^2)}{L_1C_1L_2C_2}}$$

in which f_1 is given by using the positive sign in the right-hand member f_2, the negative sign. The derivation of the values used for the constants in the equation is given in the appendix.

In the case of the principal component there is a remarkable similarity between the observed and theoretical values of frequency, the two curves coinciding except through the middle portion of the range. Although the discrepancy here is no greater than the experimental error, it is thought to be real.

The observed curve of secondary component frequencies differs considerably from the theoretical, especially for low values of capacity. The bending over and apparent flattening out of the observed curve at this end of the scale is open to some question, since for small capacities the amplitude of the secondary component is so small that no accurate measurements of it were possible.

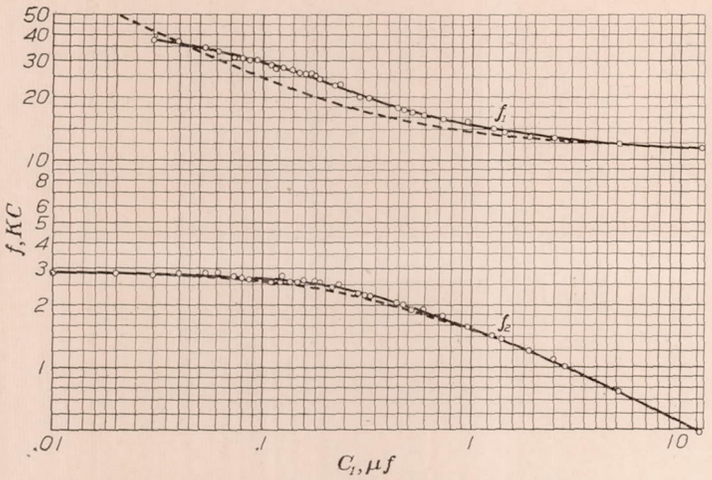

FIGURE 7.—Frequency in kilocycles per second versus primary capacity in microfarads, Northeast coil

f_1 is frequency of secondary component, i. e., that having smaller amplitude.
f_2 is frequency of principal component, i. e., that having larger amplitude.
Dotted curves show theoretical values.

With the experimental methods employed, the accuracy of any curve of secondary voltage against breaker capacity is somewhat limited. As previously mentioned, the secondary voltage is directly proportional to the current in the primary at the instant the breaker opens the primary circuit. Although a constant voltage was employed as the source of primary current, the value of the current at break varied somewhat on account of the variable contact resistance of the breaker. Thus for a given breaker capacity the secondary voltage might well vary within a range of 10 or 12 per cent. No particular accuracy is therefore claimed for the curves of Figure 8, which are presented mainly for qualitative purposes.

All four curves are of maximum voltage, i. e., V_2^+ is the maximum voltage attained by the first positive half cycle of the main wave; V_2^-, the maximum of the first negative half cycle; V_2^{++}, the maximum of the second positive half cycle; and V_2^{--}, the maximum of the second negative half cycle.

The different sections of the curves for the first two half cycles indicate the effect of the movement of the secondary component humps around the main wave, whereby first one and then another occupies the maximum position. This shift of maximum voltage from hump to hump is clearly shown in Figure 6 by comparing films PL9756 and PL9758. Counting the humps in the order of their occurrence from left to right, the maximum voltage occurs on the third hump in the former oscillogram, but on the second in the latter. This particular shift is indicated on the V_2 curve by the crossing of the first two sections of the curve at a breaker capacity of 0.062 microfarad.

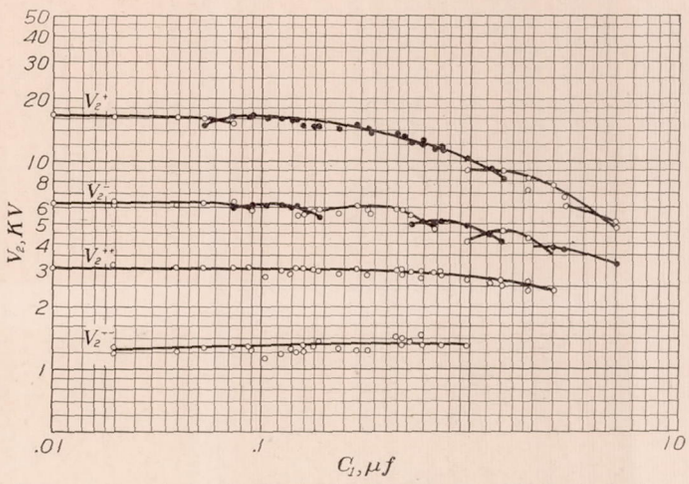

FIGURE 8.—Secondary crest voltage in kilovolts is primary capacity in microfarads, Northeast coil

V_2^+ is crest of first positive half cycle.
V_2^- is crest of first negative half cycle.
V_2^{++} is crest of second positive half cycle.
V_2^{--} is crest of second negative half cycle.

It is interesting to note that the maximum potentials of the different half cycles do not decrease at the same rate. The slight rise in the curve for the second negative half cycle is less than the probable accuracy of the graph, but in view of the same condition being found elsewhere, is considered actual.

Delco coil.—As in the previous case, great changes in the shape of the main wave were found with changes in the breaker capacity. Oscillograms were taken for some 40 different values of this capacity. Twelve of these, selected so as to best show the major changes in wave shape, are given in Figure 9. All of these oscillograms were taken with the same external adjustments of the oscillograph, so, except for slight variations due to vacuum differences, are directly comparable. There are two main wave exposures on film PL9822, the second being for the normal condition. The faintness of PL9810 is due to the under development of the original film.

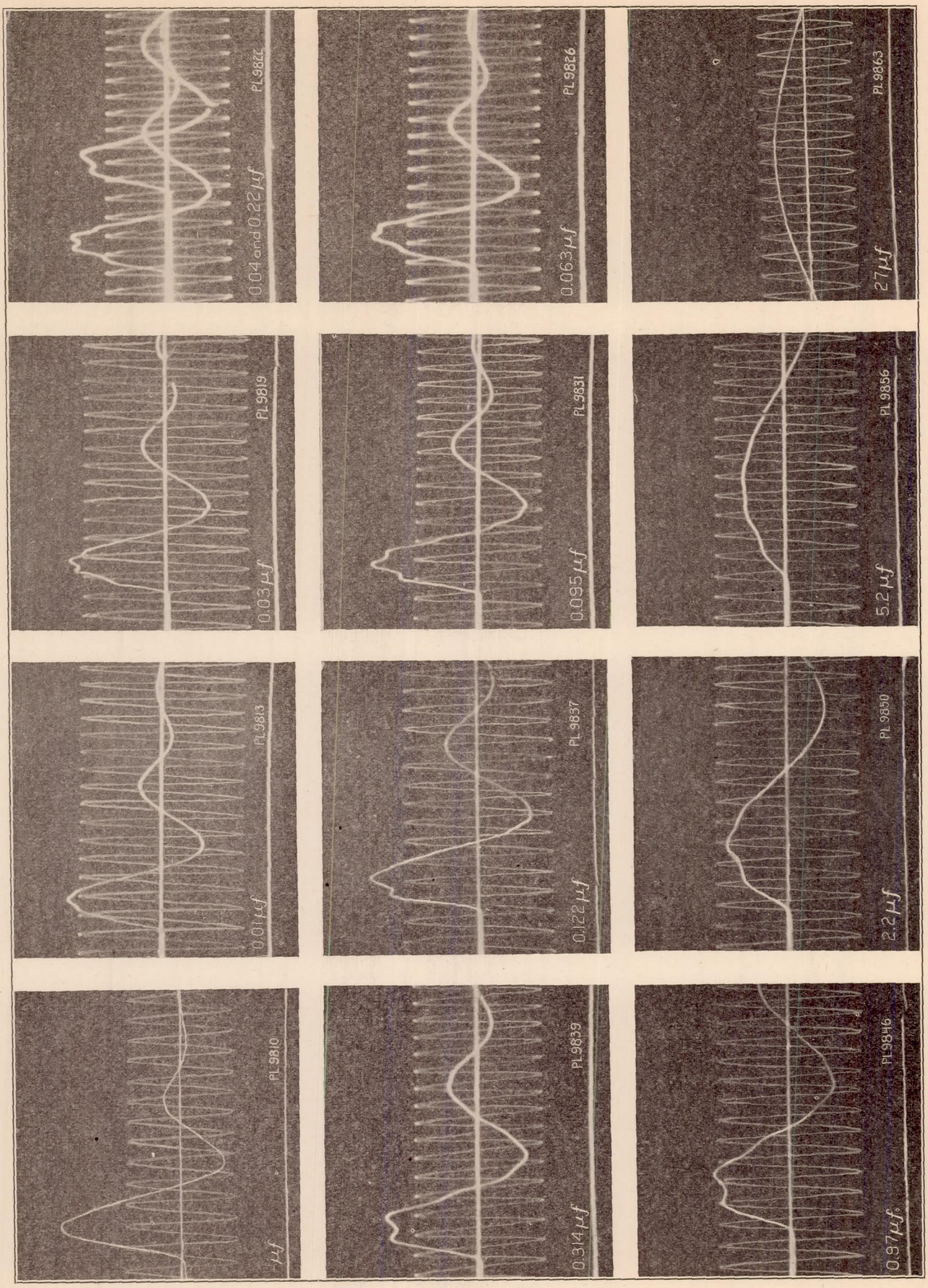

FIGURE 9.—Secondary voltage versus time for various values of primary capacity, Delco coil

The same qualitative changes in wave shape are found here as with the Northeast coil. The amplitude of the principal component steadily decreases with increase of capacity. The amplitude of the secondary component is practically zero at very large and very small values of capacity, reaching a maximum at some intermediate value around 0.122 microfarad.

The frequency of the principal component drops continuously, as does that of the secondary component. With increasing values of capacity up to about 0.97 microfarad the frequency of the secondary component decreases more rapidly, beyond this value more slowly, than does that of the principal component.

Curves of observed and theoretical frequencies as given by the equation of the previous section) are shown in Figure 10. As previously, the continuous curves are approximations of the measured values shown by the small circles; the dotted curves, the theoretical values. With both components there is

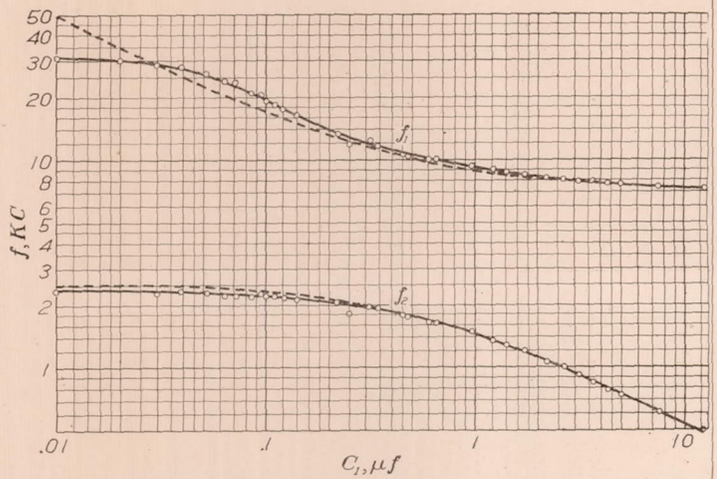

FIGURE 10.—Frequency in kilocycles per second versus primary capacity in microfarads, Delco coil

f_1 is frequency of secondary component, i. e., that having smaller amplitude.
f_2 is frequency of principal component, i. e., that having larger amplitude.
Dotted curves show theoretical values.

good agreement between theory and observation. The discrepancy at small values of breaker capacity in the case of the principal component may well be due to the fact that the main wave really oscillates not about the true zero line, but about a downward sloping exponential which is slightly above, and ultimately joins with, the zero axis. According to Silsbee (Reference 8), who predicted this fact, it is due to the presence of eddy currents in the iron core. The effect of such action is to cause the apparent frequency of the first half cycle (computed from measurements along the zero axis) to be less than that of the second, which in turn is greater than that of the third, and so on. Measurements were made in all cases of the apparent frequencies of each of the first four half cycles, although only that of the first is plotted. For small values of capacity the difference between the measured frequencies of the first and second half cycles was about 10 per cent, that of the second half cycle being always the greater.

Curves of maximum voltage attained by each of the first four half cycles are shown in Figure 11. The notation is the same as previously employed. With the first negative half cycle, the shifts of maximum voltage from hump to hump were too indistinct to follow. Two such shifts occurred in the first positive half cycle, although the second, which occurred at the end of the range, is not indicated. The shift shown by the intersection of the two sections of the curve at 0.043 microfarad can be seen by comparing films PL9822 and PL9826 of Figure 9. In film PL9822 the maximum voltage occurs on the third hump, in film PL9826 on the second. In this case the rise in maximum voltage of the third and fourth half cycles is very apparent.

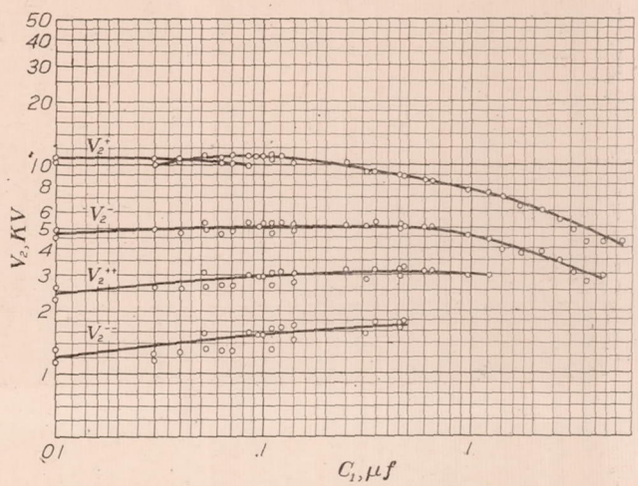

FIGURE 11.—Secondary crest voltage in kilovolts versus primary capacity in microfarads, Delco coil

V_2^+ is crest of first positive half cycle.
V_2^- is crest of first negative half cycle.
V_2^{++} is crest of second positive half cycle.
V_2^{--} is crest of second negative half cycle.

SERIES WITH VARYING SHUNTED SECONDARY CAPACITY

Northeast coil.—Oscillograms were taken for 17 different values of shunted secondary capacity. As to be expected, considerable resultant change in wave shape was observed. Oscillograms for 13 different values of capacity are shown in Figure 12. The value of capacity marked at the bottom of each picture gives the total effective capacity with which the film was taken. This value includes the distributed capacity of the coil itself, 57 micromicrofarads, and the capacity of the deflecting plates of the oscillograph, 23 micromicrofarads. The method employed to find the distributed capacity of the coil is given in the appendix.

In film PL9901 the complete wave is photographed in two sections. The first section, taken in the usual manner, begins as usual with the first positive half cycle, which appears as the one of greatest magnitude, and ends with the close of the second positive half cycle, at which instant the cathode beam passed off the film. The second section of the wave was taken

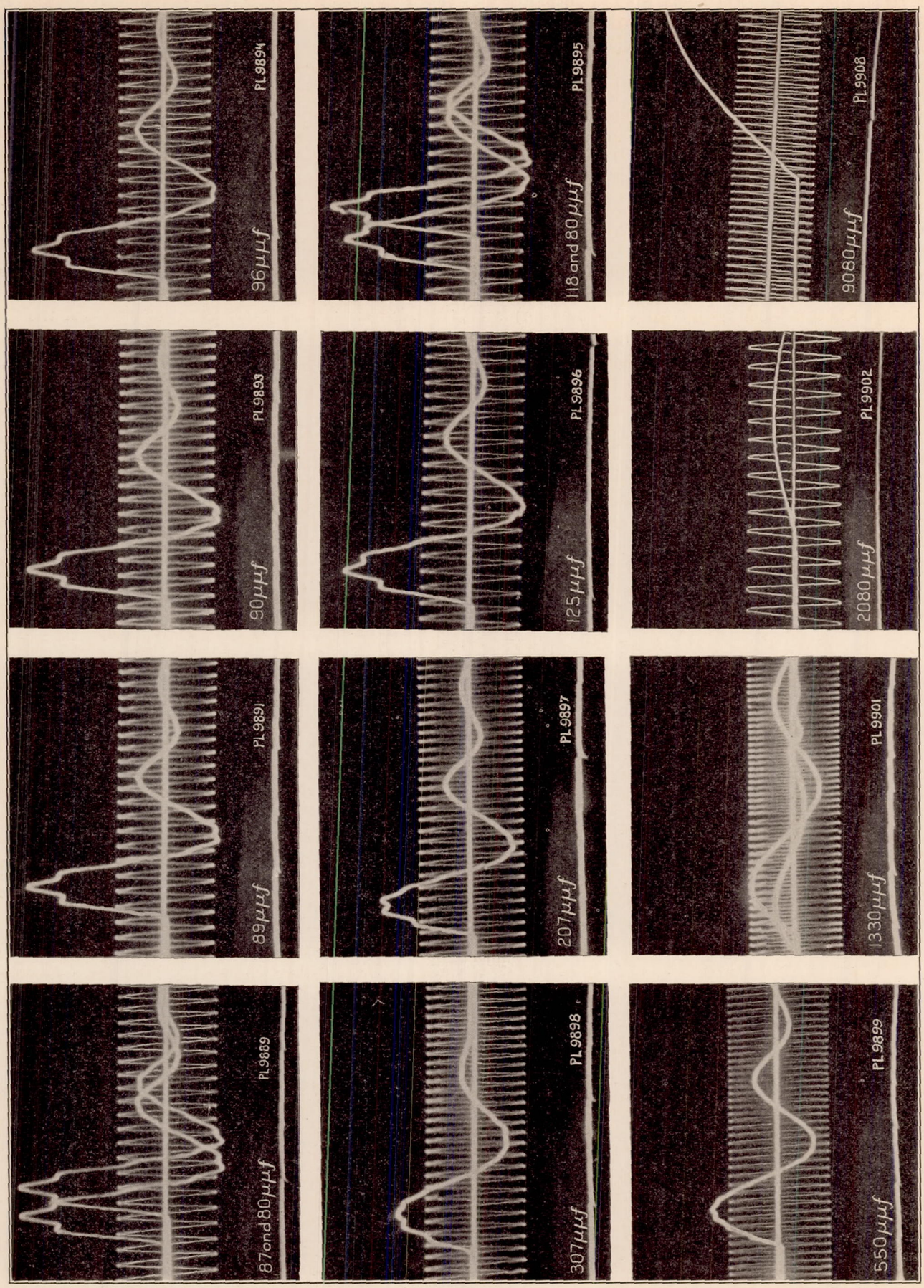

FIGURE 12.—Secondary voltage versus time for various values of secondary capacity, Northeast coil

after the stator of the breaker-driving motor had been sufficiently advanced so that at the instant the cathode beam entered on the film the secondary voltage wave had already gone through one positive and one negative half cycle. The second section thus begins with the second positive half cycle, which can be seen below and a little to the left of the first positive half cycle of the other section.

Various sweeping speeds were used in taking the films shown in Figure 12 as indicated by the crowded or open appearance of the timing wave, which in every case had a frequency of 15 kilocycles. Adjustment for voltage deflection was the same in all films except the last, which has a deflection for a given voltage approximately six times as great as the others.

An inspection of the series indicates that the frequency of the principal component decreases steadily with an increase of capacity. Since the humps of the secondary component move counterclockwise it is impossible to tell without measurement whether the frequency of the secondary component decreases or not. It is certain, however, that if it does decrease, it does so at a rate less than that of the principal component.

The amplitude of both components clearly decreases with an increase of capacity. It is interesting to speculate whether with values of capacity less than the minimum here obtainable, the amplitude of the secondary component would decrease.

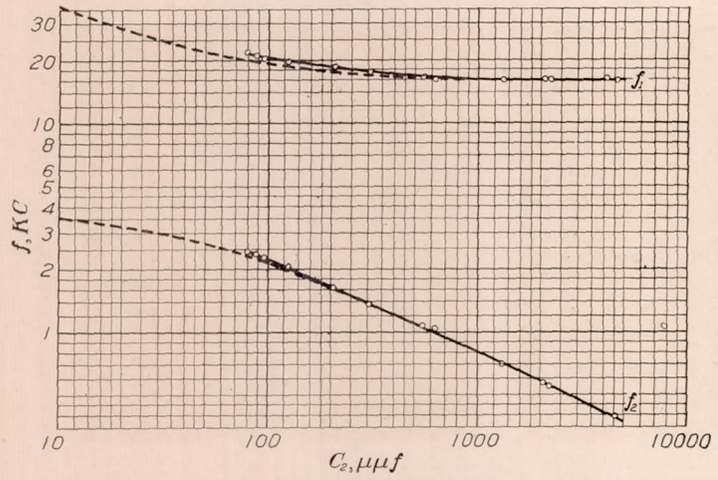

FIGURE 13.—Frequency in kilocycles per second versus secondary capacity in micromicrofarads, Northeast coil

f_1 is frequency of secondary component, i. e., that having smaller amplitude.
f_2 is frequency of principal component, i. e., that having larger amplitude.
Dotted curves show theoretical values.

Curves of the frequencies of the two components are given in Figure 13. The values of secondary capacity for which observed frequencies are plotted include in every case the distributed capacity of the ignition coil and the capacity of the deflecting plates. The values on the graph thus represent the sum of these two and the external capacities used.

Here also there is a very good agreement between the observed and theoretical values of frequencies. The theoretical frequencies were found by using the same equation as was employed in the previous sections and are shown by the dotted curves.

The discrepancies at small values of capacity may possibly be due to error in the value found for the distributed capacity of the ignition coil. Since this was added to the value of external capacity to obtain the value plotted, a small error in its determination would cause appreciable distortion of the curve at the bottom of the range.

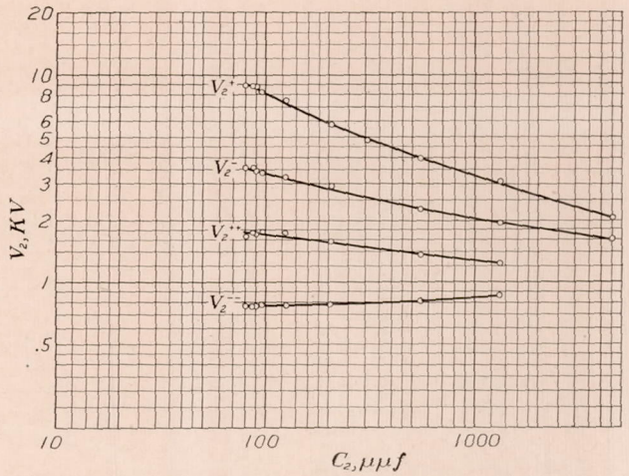

FIGURE 14.—Secondary crest voltage in kilovolts versus secondary capacity in micromicrofarads, Northeast coil

V_2^+ is crest of first positive half cycle.
V_2^- is crest of first negative half cycle.
V_2^{++} is crest of second positive half cycle.
V_2^{--} is crest of second negative half cycle.

Curves of the maximum voltage attained by each of the first four half cycles are shown in Figure 14. In plotting these curves only those films taken during the same run were used, as the remaining few in the series, taken at a later date, gave points considerably off the curves shown. This is the natural result of the impossibility of maintaining constant current conditions in the primary circuit. Incidentally it is interesting to notice that, as shown in Figure 3, these changes in primary current have no effect upon the frequencies.

These voltage curves for secondary capacity are in the main similar to those of Figure 8, which are for primary or breaker capacity. They are, however, much steeper, indicating that a proportionate increase of capacity in the secondary circuit causes a greater drop in maximum voltage than does the same proportionate change in the primary circuit. In the case of secondary capacity the effect of the maximum voltage of the first half cycle shifting from hump to hump is small, since by the time such a shift occurs the amplitude of the secondary component is small. Such shifts are accordingly not shown.

Delco coil.—Oscillograms for 13 of the 17 values of secondary capacity used in the series are shown in Figure 15. The distinct breaks in several of the main voltage waves, notably the left-hand wave of film

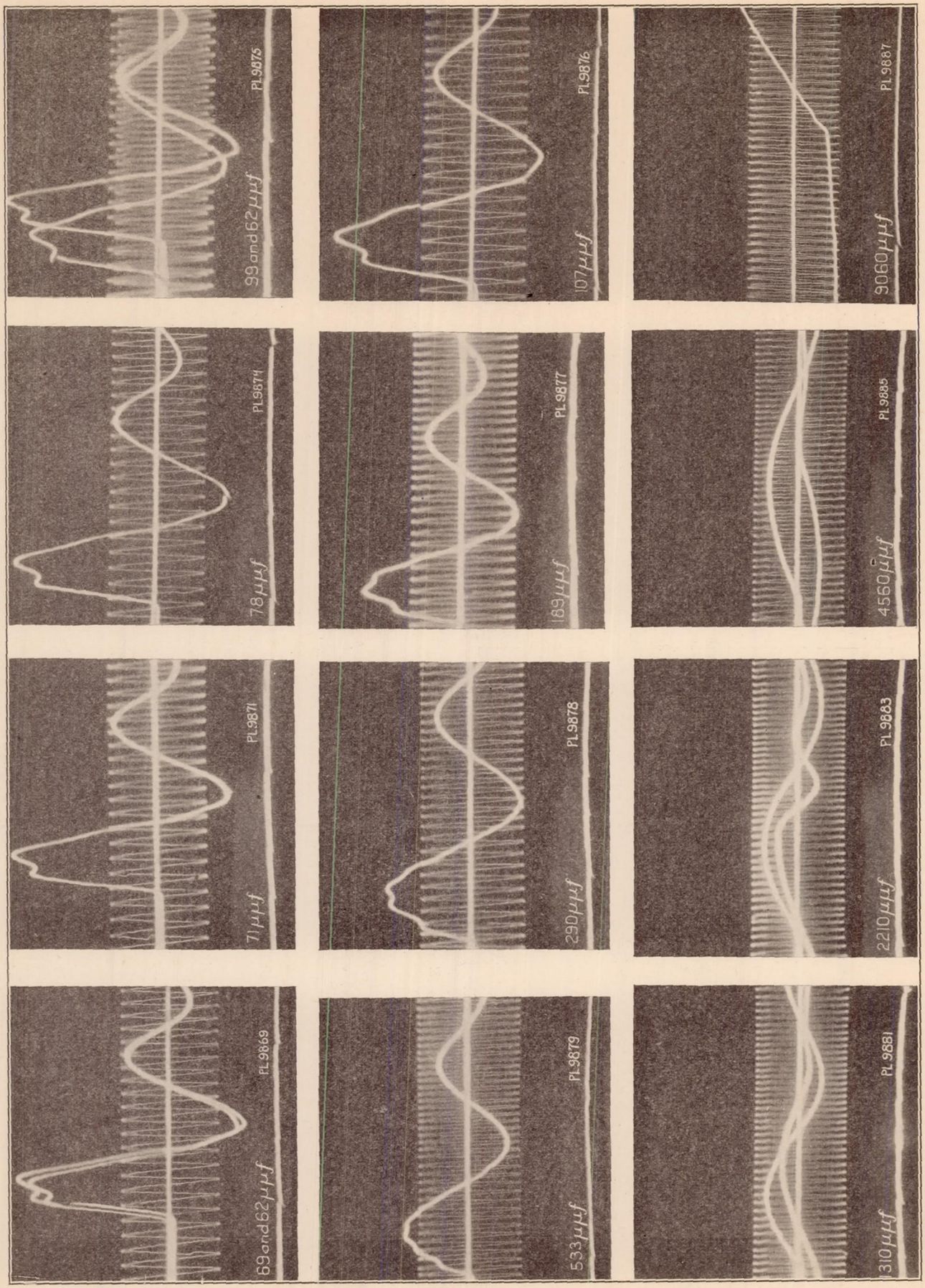

FIGURE 15.—Secondary voltage versus time for various values of secondary capacity, Delco coil

PL9875, have nothing to do with the waves themselves, but were caused by momentary interruptions in the electron emission of the cathode. On the first three films in the bottom row the wave was photographed in two sections.

The result of photographing two sections of the same wave on the same film is brought out most clearly in film PL9885. In this film the first section consists of the first positive half cycle and a small portion of the first negative half cycle. The second section begins at approximately the point where the first section ended, and included the first negative half cycle. At the end of the first negative cycle the breaker in the primary circuit closed, causing the remaining energy available for oscillations in the secondary to be rapidly dissipated. This is shown by the fact that although the amplitude of the first negative half cycle is considerable, there is no appreciable subsequent oscillation. The same effect occurs in film PL9883, where the breaker closed at the instant the main wave was approximately at the peak of the second positive half cycle. At this point the main wave broke, and from there on oscillated with a very different frequency.

The usual qualitative relationships are apparent from Figure 15. The frequency and amplitude of the principal component decrease continuously with an increase of capacity. The amplitude of the secondary component also decreases with an increase of capacity

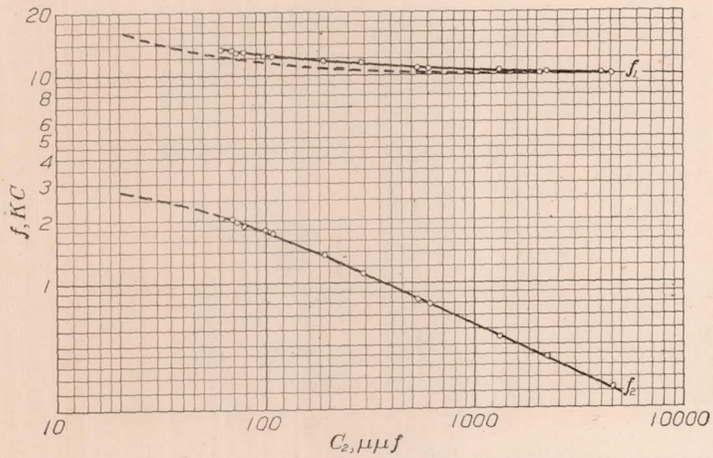

FIGURE 19.—Frequency in kilocycles per second versus secondary capacity in micromicrofarads, Delco coil

f_1 is frequency of secondary component, i. e., that having smaller amplitude.
f_2 is frequency of principal component, i. e., that having larger amplitude.
Dotted curves show theoretical values.

while the frequency, if it does decrease, does so at a rate slower than that of the principal component.

An interesting point not mentioned before is shown by reference to film PL9887. On this film, at the instant the breaker opened the primary circuit (indicated by the arrow) the secondary voltage was clearly opposite to that induced after the break. This condition was true of all films, and is due to the fact that at the high breaker speeds employed the current in the primary circuit did not reach its steady state value, but was always increasing when interrupted by the breaker. Thus previous to the opening of the breaker there was a negative induced voltage in the secondary.

Curves of the observed and theoretical frequencies are shown in Figure 16. The values of capacity for which the observed frequencies are plotted are the total effective capacities, which in every case include the distributed capacity of the ignition coil, 38 micromicrofarads; and the capacity of the deflecting plates, 23 micromicrofarads. The continuous curve is that of the observed frequencies; the dotted, of the theoretical. The theoretical curve was obtained by the same equation previously used.

A beautiful agreement is evident between the theoretical and observed frequencies of the principal component, the two curves coinciding exactly over the entire range.

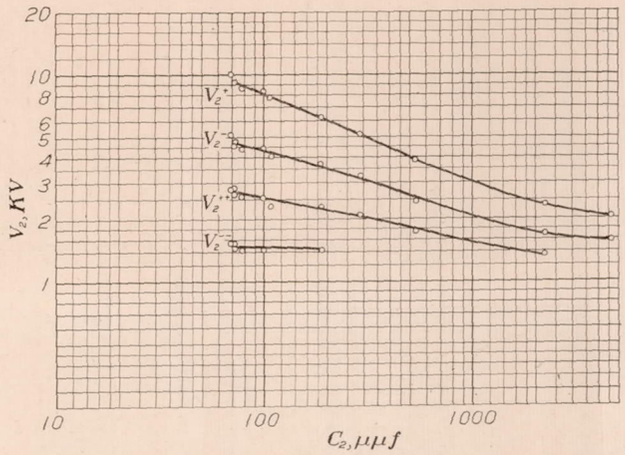

FIGURE 17.—Secondary crest voltage in kilovolts versus secondary capacity in micromicrofarads, Delco coil

V_2^+ is crest of first positive half cycle.
V_2^- is crest of first negative half cycle.
V_2^{++} is crest of second positive half cycle.
V_2^{--} is crest of second negative half cycle.

The familiar voltage curves for the series are shown in Figure 17. As in the frequency curves, the values of capacity for which observed voltages are plotted are in every case total effective values.

SERIES WITH VARYING SHUNTED SECONDARY RESISTANCE

Northeast coil.—Twenty-three different values of shunted secondary resistance were used in taking the oscillograms of this series. Oscillograms for 13 such are shown in Figure 18. The films in this series are directly comparable except that the voltage scale of the last two is one-sixth as great as the others.

The second main wave, on the first film, PL9700, marked for a resistance of $1{,}100 \times 10^4$ ohms, is the wave for the normal condition, that value of resistance being the standard. Incidentally the values marked at the bottom of the oscillograms are those of the external shunts with which the pictures were made,

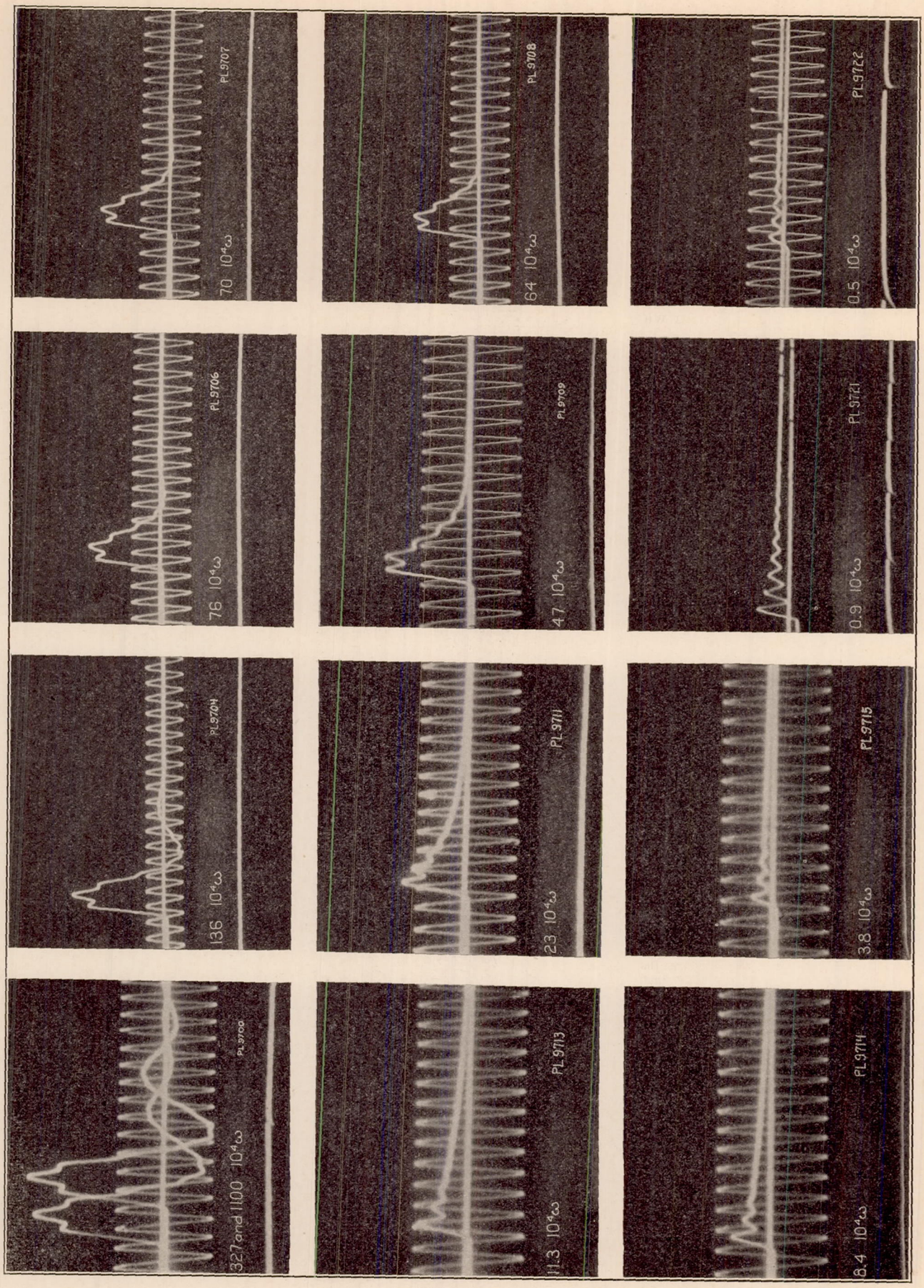

FIGURE 18.—Secondary voltage versus time for various values of resistance shunting the secondary, Northeast coil

and do not include the internal resistance of the secondary winding.

It is at once apparent from Figure 18 that the oscillatory nature of the principal component is soon lost, the wave failing to pass below the zero line for values of resistance less than 64×10^4 ohms. On the other hand, the secondary component continues to oscillate to the end of the range, and even there gives no indication of increased damping.

The amplitude of both components decreases as the resistance of the shunt decreases, but that of the principal component seems to change more rapidly. When the principal component is damped out of oscillation, the main wave becomes simply the secondary component oscillating about an exponential impulse.

Curves of the observed frequencies of the two components are given in Figure 19. The values of resistances used in plotting observed points are simply those of the external shunts employed. The term "frequency" has a questionable meaning when applied to the principal component at values of resistance below 1.36 megohms, for which properly speaking, there is no oscillation. The frequency of the main component plotted for such values of resistance, is the frequency of a wave, the time for one-half cycle of which is the same as the time taken by the main wave to pass from zero back to zero.

For the purpose of comparison, the corresponding frequency curves of the Delco coil are plotted with

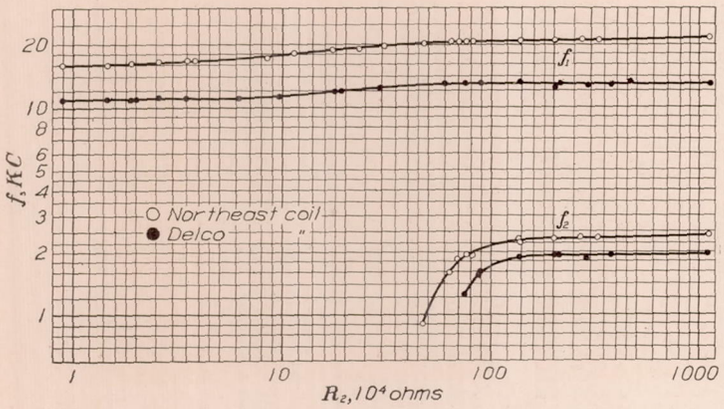

FIGURE 19.—Frequency in kilocycles per second versus secondary shunting resistance

f_1 is frequency of secondary component, i. e., that having smaller amplitude.
f_2 is frequency of principal component, i. e., that having greater amplitude.

those of the Northeast coil in Figure 19. It is apparent that the frequencies of both coils vary according to the same law. As a very large capacity affects a circuit in somewhat the same way as does a very low resistance, it is logical to suppose that the frequency of the secondary oscillations of a coil shunted by a large capacity would approach the value of those existing in the coil when it was shunted by a low resistance. A comparison of the secondary component frequencies given in Figure 19 for low values of shunted resistance, with the secondary component frequencies given by Figures 13 and 16 for large values of shunted capacity, shows that this relationship holds for both coils.

Figure 20 gives the curves of the maximum voltage attained by each of the three first half cycles. As the main wave is damped out of oscillation, the third and second half cycles rapidly disappear, while the first half cycle becomes an impulse. The familiar shifting

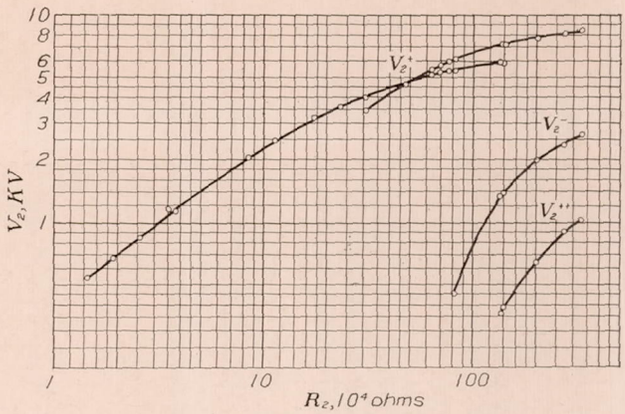

FIGURE 20.—Secondary crest voltage in kilovolts versus secondary shunting resistance, Northeast coil

V_2^+ is crest of first positive half cycle or impulse.
V_2^- is crest of first negative half cycle.
V_2^{++} is crest of second positive half cycle.

of the maximum voltage of the first half cycle from hump to hump is shown in the curve for the maximum voltage of that half cycle, as well as in films PL9709 and PL9711 of Figure 18. In PL9709 the maximum occupies the second hump, in PL9711 the first.

Delco coil.—In this series oscillograms were taken with 23 different values of shunted secondary resistance. Twelve films, embodying 13 of these are shown in Figure 21. The sweeping speed is approximately the same in all cases shown, but the deflection for a given voltage is six times as large in the last two films, PL9739 and PL9743, as it is in the others. The second wave in the first film, PL9723, marked for a shunted resistance of 1100×10^4 ohms, is the voltage wave for the normal condition.

The variations in the shape of the main wave are qualitatively the same as those found under similar conditions with the Northeast coil. The principal component is rapidly damped out of oscillation, but the secondary component continues to oscillate with only a slight diminution of frequency over the entire range. The amplitude of the principal component drops off more rapidly than does that of the secondary component.

The frequency curves for the two components have been given in Figure 19. The values of resistances used in plotting the curves include only the resistance of the external shunt. As in every case with similar

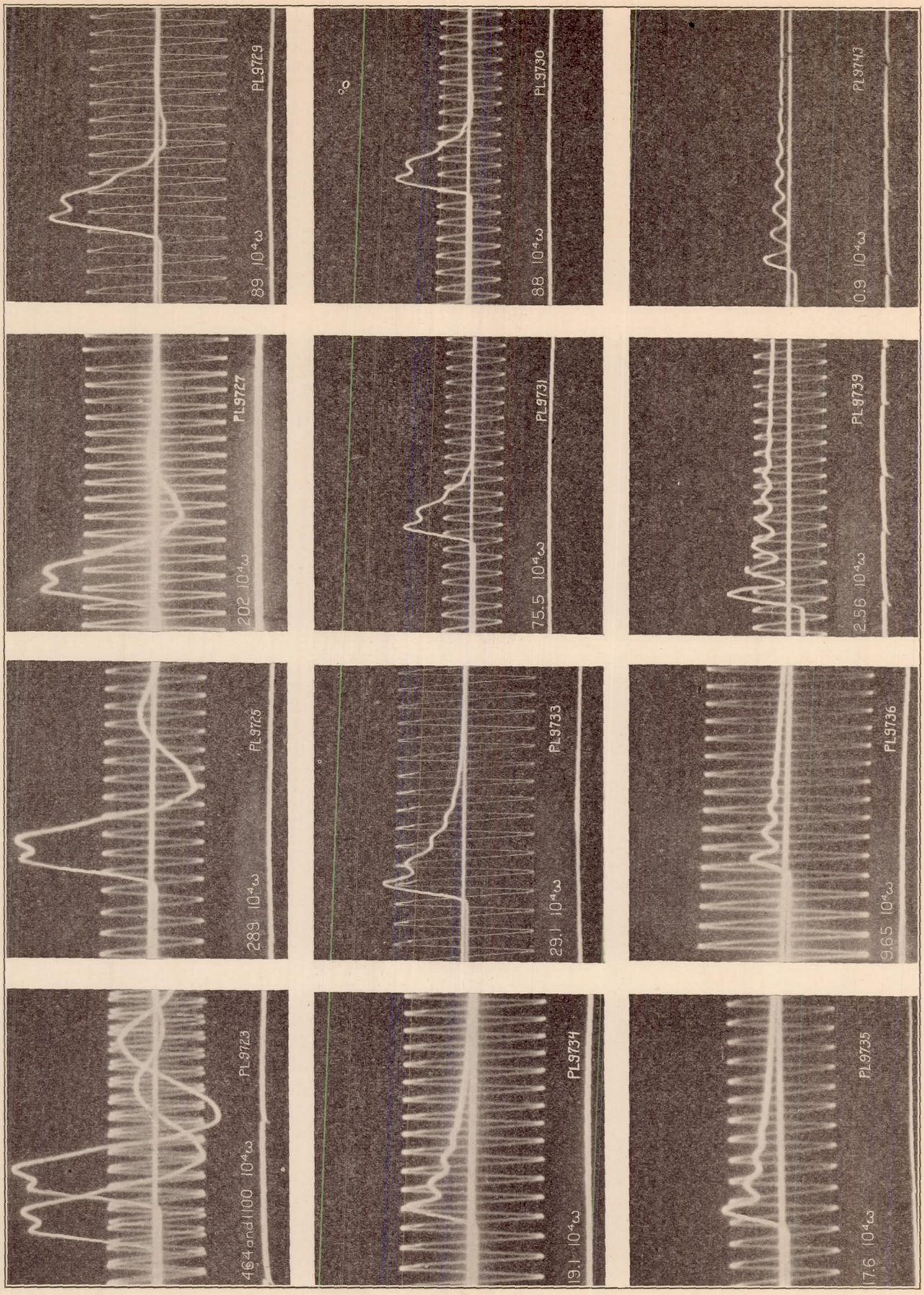

FIGURE 21.—Secondary voltage versus time for various values of resistance shunting the secondary, Delco coil

external conditions, the frequencies of the Delco coil are less than those of the Northeast.

The voltage curves are shown in Figure 22. The shift of maximum voltage from hump to hump indicated by the break in the curve for the first positive half cycle is shown in films PL9725 and PL9727 of Figure 21, in which the maximum is seen to pass from the second to the first hump.

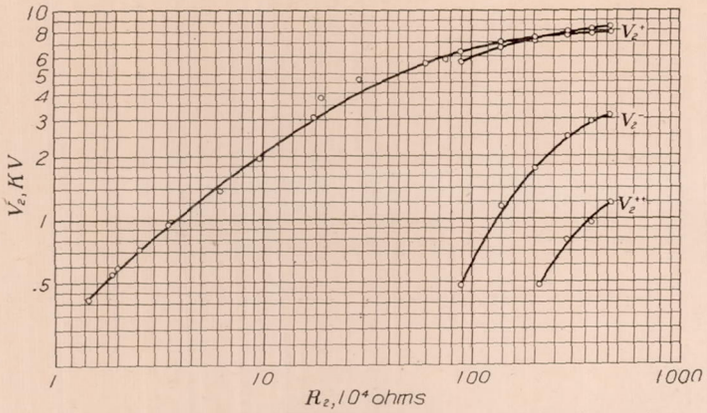

FIGURE 22.—Secondary crest voltage in kilovolts versus second shunting resistance, Delco coil

V_2^+ is crest of first positive half cycle or impulse.
V_2^- is crest of first negative half cycle.
V_2^{++} is crest of second positive half cycle.

SECONDARY VOLTAGE-PRIMARY CURRENT OSCILLOGRAMS

The secondary voltage-primary current oscillograms are probably more fantastic in appearance than any of the others. Typical examples are shown in Figures 23 and 24, which figures should be viewed with the long dimension of the sheet horizontal. Considering now Figure 23. The film on the right, PL9962, contains four separate exposures. The straight horizontal line across the center of the film is the zero voltage reference axis; the straight horizontal line across the lower part of the film, the voltage calibration line. The straight vertical line down the right side of the film is the current calibration line. No zero current reference axis was placed on the film, but if it had been, it would appear as a straight vertical line passing down through the center of the film.

In taking the curve PL9962 no time displacement of any sort was employed. The oscillograph was adjusted so that the secondary voltage caused vertical displacements of the cathode beam, while the primary current caused horizontal displacements. Thus points on the curve indicate simultaneous values of the voltage across the secondary winding and the current in the primary circuit.

To have the oscillograph record fluctuations in the primary current, it was necessary to connect one set of the oscillograph deflecting coils in series with the primary circuit. The effect of the shape of the secondary voltage wave of introducing such external inductance into the primary circuit is seen by comparing film PL×9745 of Figure 23, with film PL×9718 of Figure 2. Both are for the normal condition of the Northeast coil, except that in taking the former the deflecting coils of the oscillograph were connected in the primary circuit.

The films of Figure 24 are thus directly comparable, similarly marked points on each being the same. Film PL9981 shows that at the instant the breaker opened the primary circuit (point 1) the current in the primary had a relatively high value, while the secondary voltage was slightly negative. After the instant of break, the current dropped rapidly, passed through zero into negative values, and was coming up through zero for the second time as the voltage reached its first maximum (point 2), and so on.

It is now apparent that a secondary voltage-primary current oscillogram gives both the value of the current interrupted in the primary circuit, and the maximum value of the resultant secondary voltage. Series of such oscillograms were taken with varying values of interrupted primary current. The data from the series are plotted as the solid circles of Figures 4 and 5.

Oscillograms of the primary current versus time for the condition of the same set of deflecting coils being in the primary circuit, are shown in Figure 25. The straight horizontal line across the center of each film is the line of zero current; the straight horizontal line across the lower portion, the current calibration line.

A comparison of these curves shows the distorting effect of an arc across the breaker points. With the deflecting coils in the primary circuit, both ignition coils showed approximately the same primary current versus time oscillogram for clean interruptions of the breaker. The difference between the films shown is due to the arc which occurred across the breaker when film, PL×9741, was made.

CONCLUSIONS

The main conclusion to be drawn from the investigation is that, qualitatively at least, there is very little about the electrical features of the operation of an ignition coil which has not been explained and predicted by mathematical theory. Quantitatively, actual results differ somewhat from the theoretical, although as here shown, in the case of the component frequencies of the secondary voltage wave, there is excellent agreement.

It is realized that the present analysis of the experimental evidence is incomplete. Particularly is this true of the secondary voltage-primary current oscillograms, which contain a great deal more of value than the relationship between interrupted primary current and maximum resultant secondary voltage. In the limited time available the most obvious points were developed, and such are presented. It is felt, however,

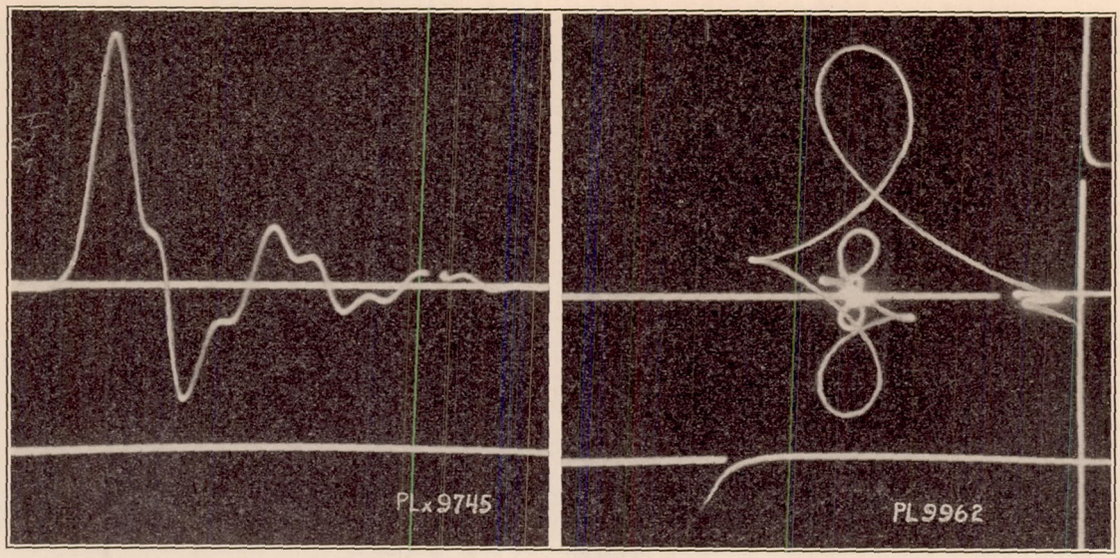

FIGURE 23.—Secondary voltage versus time (PL 9745) and secondary voltage versus primary current (PL 9962) for Northeast coil, normal conditions

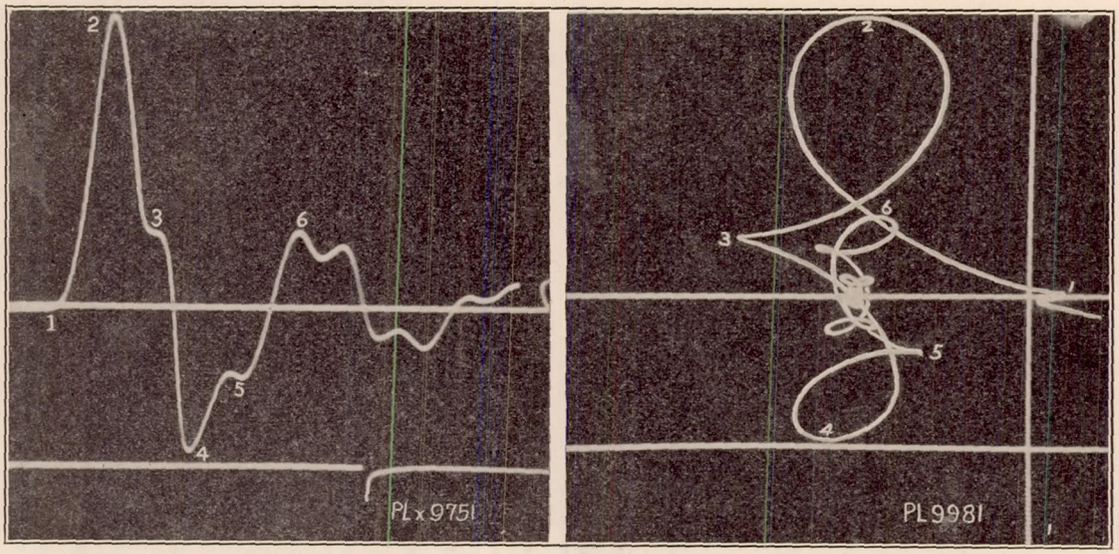

FIGURE 24.—Secondary voltage versus time (PL 9751) and secondary voltage versus primary current (PL 9981) for Delco coil, normal conditions

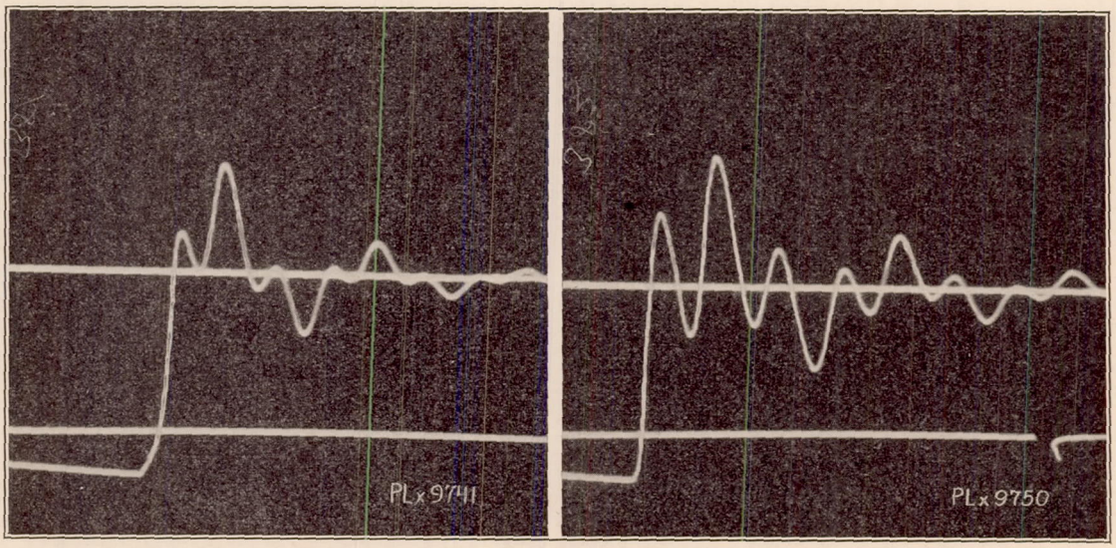

FIGURE 25.—Primary current versus time for the Northeast (PL 9741) and Delco (PL 9750) coils

that the main objective of the undertaking, to obtain a qualitative check on the theory, was achieved.

A word as to the accuracy of the quantitative results. The oscillograph employed is known to be such a faithful reproducer that errors due to it are negligible. Measurements on the oscillograms were made to a quarter of a millimeter, and all were checked at least twice, many three or four times. The general over-all accuracy, including the approximations of method, is thought to be within 5 or 6 per cent.

ACKNOWLEDGMENTS

The author acknowledges his gratitude to the officials of the lightning arrester department of the General Electric Co. for placing their laboratory at his disposal; to the laboratory staff for much assistance in setting up and operating the equipment; to Dr. F. B. Silsbee, of the Bureau of Standards, for the measurements of certain coil constants, but especially for the helpful advice, suggestions, and encouragement given throughout the work.

Thanks are also extended to the manufacturers who provided the ignition apparatus, and to Doctor Dahl, of the Massachusetts Institute of Technology, who has acted as official advisor to the work.

APPENDIX

MEASUREMENT OF COIL CONSTANTS

The following constants of an ignition coil are necessary in computing its performance.

L_1 = the inductance of the primary winding.
L_2 = the inductance of the secondary winding.
M = the mutual inductance between windings.
k = the coefficient of coupling, equal to $\sqrt{\frac{M^2}{L_1 L_2}}$
r_1 = the resistance of the primary winding.
r_2 = the resistance of the secondary winding.

The values of these constants for both coils were found by measurements made at the Bureau of Standards in Washington, D. C. The resistances were measured in the regular manner on a wheatstone bridge. The mutual inductances were measured by Dr. F. B. Silsbee, physicist of the bureau, using a fluxmeter. The remaining three constants were obtained by first finding the transformation ratios of the coils.

The method employed to find the transformation ratios, which is fully described in an N. A. C. A. Report (Reference 9), is shown schematically in Figure 26. S and P are respectively the secondary and primary windings of the ignition coil; R_1, R_2, R_3, and R_4 are noninductive adjustable resistances; B is a battery; and G is sensitive ballistic galvanometer. R_3 and R_4 were adjusted until there was no deflection of the galvanometer with a steady current flowing through the primary winding. R_1 and R_2 were then adjusted until there was no throw of the galvanometer when this current was interrupted. When a balance had been obtained under both conditions, the transformation ratio was given by

$$n_p = \frac{r_2 + R_1}{r_1 + R_2}$$

Using the same procedure with current flowing through the secondary winding, Figure 26b, another ratio was obtained,

$$n_s = \frac{r_2 + R_1'}{r_1 + R_2'}$$

It is also shown in the report above referred to, that

$$n_p = \frac{M}{L_1} \text{ and } n_s = \frac{L_2}{M}$$

Whence

$$L_1 = \frac{M}{n_p} \text{ and } L_2 = n_s M$$

Also

$$k^2 = \frac{M^2}{L_1 L_2} = \frac{n_p}{n_s}$$

The values of M obtained for different values of current in the primary windings are shown plotted in Figure 27. The average maximum voltages for the normal conditions of the Northeast and Delco coils were respectively 9 and 10 kilovolts. From $V_2 I_1$ curves of Figures 4 and 5, these voltages indicate primary currents of 1.6 and 1.5 amperes. The values of M corresponding to these currents were taken to be the most representative. The values L_1, L_2, M, K^2, N_r, N_s, R_1, and r_2 are given in Table I.

The value of the distributed capacity of the secondary of the ignition coil was found from the observed curve of component frequencies versus breaker capacity. E. Taylor-Jones shows (Reference 10) that as the breaker capacity approaches infinity, the frequency

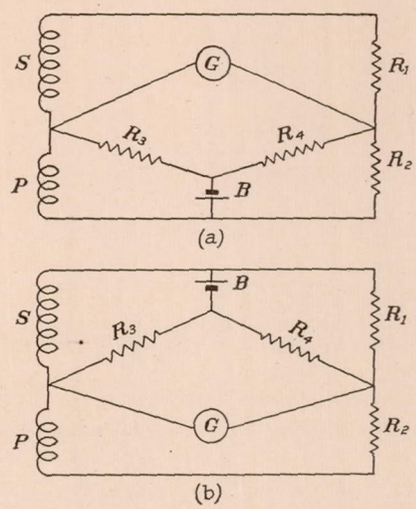

FIGURE 26.—Circuits used in determining the effective turn ratio of the coils

of the principal component becomes zero, and that of the secondary component,

$$f_1 = \frac{1}{2\pi\sqrt{L_2 C_2 (1 - k^2)}}$$

Assuming that the frequency at the end of the observed curve is not much different from that for an infinite capacity, and using the value shown on the curve (fig. 7), we have for the Northeast coil,

$$11{,}700 = \frac{1}{2\pi\sqrt{L_2 C_2 (1 - 0.938)}}$$

Whence

$$L_2 C_2 = 30 \times 10^{-10}$$

and using the value of L_2 given in Table I,

$$C_2 = 79.8 \mu\mu f.$$

Subtracting the known value of capacity of the deflecting plates, $23 \mu\mu f$, leaves the distributed capacity of the secondary of the coil,

$$c = 57 \mu\mu f.$$

A similar procedure for the Delco coil gives

$$L_2C_2 = 38.7 \times 10^{-10}$$
$$C_2 = 61.3 \mu\mu f.$$

And

$$c = 38 \mu\mu f.$$

The values of L_2C_2 given above were used in finding the theoretical component frequencies plotted as the dotted lines in Figures 7 and 10.

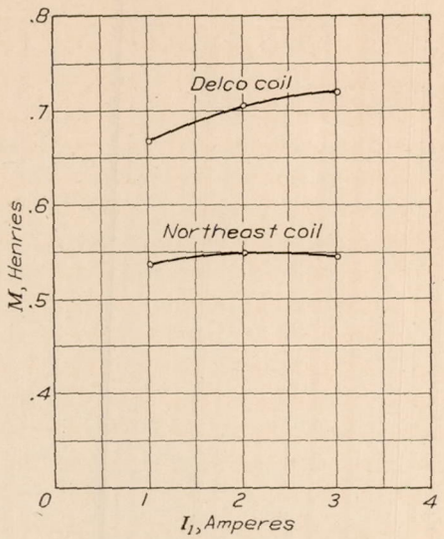

FIGURE 27.—Effective mutual inductance between primary and secondary windings as a function of primary current

MEASUREMENT OF CIRCUIT CONSTANTS

The capacities of the condensers used across the breaker were measured on a General Radio capacity bridge.

The capacities of the condensers used across the secondary winding were measured by a General Radio precision wave meter. The method was to tune the wave meter to resonance with the output of a laboratory oscillator, shunt the condenser to be measured across the wave-meter condensor, and note the reduction in capacity of the wave-meter condenser necessary to bring the wave meter once more in resonance. The wave-meter condenser being a calibrated one, the capacity of the condenser in question was obtained with high accuracy.

The resistances of the water tube shunts employed across the secondary were measured on a Wheatstone bridge, both immediately before, and immediately after use.

MEASUREMENT OF COMPONENT FREQUENCIES GIVEN BY OSCILLOGRAMS

In measuring the frequency of the principal component, the effect of the secondary component on the main wave was neglected; that is, the apparent frequency of the main wave was taken as the frequency of the principal component. This introduces some error, but as the magnitude of the secondary component is relatively small, and the ratio of component frequencies never less than six, the maximum possible error in any one-half cycle of the main wave is not greater than 6 or 7 per cent. As previously mentioned, each half cycle of the main wave was measured separately.

If

mf_k = the horizontal distance covered by n cycles of the timing wave.
f_k = the frequency of the timing wave.
mf_2 = the distance between the points at which a half cycle of the main wave crossed the zero axis.
f_2 = the frequency of the half cycle of the main wave.

Then

$$f_2 = \frac{0.5}{n} \frac{f_k\, mf_k}{mf_2}$$

Usually five cycles of the timing wave were used, the ones covering the same portion of the film as the half cycle of the main wave being chosen for measurement. When the half period of the main wave became long, the number of cycles of the timing wave was correspondingly increased.

In measuring the secondary component frequencies, the secondary component humps on the main wave were taken to represent maxima of the secondary component. This method also introduces approximations, but as long as enough cycles are used the error is small. If then

mf_k = horizontal distance covered by n cycles of the timing wave.
f_k = frequency of the timing wave.
mf_1 = horizontal distance covered by p cycles of the secondary component.
f_1 = frequency of the secondary component.

Then

$$f_1 = \frac{p}{n} \frac{f_k\, mf_k}{mf_1}$$

Measurements of the oscillograms for frequency determination were made to the quarter of a millimeter. At first appearance this may seem excessive and optimistic accuracy, but after much practice such accuracy was possible and the results could be checked. Measurements were made with the original films, which were placed on a sheet of millimeter cross-section paper illuminated from the under side.

MEASUREMENT OF VOLTAGES ON OSCILLOGRAMS

Voltage determinations were extremely simple.

If

mV_k = the vertical distance between the zero axis and the voltage calibration line.

V_k = the calibration voltage.

mV_x = the vertical distance between any point on the main wave and the zero axis.

V_x = the voltage at the point.

Then

$$V_x = \frac{V_k}{mV_k} mV_x$$

JULY 24, 1930.

TABLE I

Constant	Northeast	Delco
M	0.546 henry.	0.689 henry.
n_r	65.	80. 5
n_s	69. 3.	91. 5
L_1	0. 0084 henry.	0.00856 henry.
L_2	37. 8 henries.	63.1 henries.
L_2C_2	$30\times10.^{-10}$	$38.7\times10.^{-10}$
c	$57\mu\mu f.$	$38\mu\mu f.$
k_2	0. 938.	0.88.
r^1	1.195 ohms.	1.415 ohms.
r_2	3,151 ohms.	4,115 ohms.

REFERENCES

Reference 1. Taylor-Jones, E.: Phil. Mag., 19, p. 713; 1909.

Reference 2. Taylor-Jones, E.: Phil. Mag., 14, p. 238; 1907.

Reference 3. Campbell, N. R.: Phil. Mag., 37, p. 284; 1919.

Reference 4. McEachron, K. B., and Wade, E. J.: G. E. Rev., 28, p. 622; 1925.

Reference 5. Brode, R. B., Randolph, D. W., and Silsbee, F. B.: Electrical Characteristics of Spark Generators for Automotive Ignition. N. A. C. A. Technical Report No. 241; 1926.

Reference 6. Taylor-Jones, E.: Phil. Mag., 29, p. 1; 1915.

Reference 7. Taylor-Jones, E., and Roberts, D. E.: Phil. Mag., 22, p. 706; 1911.

Reference 8. Silsbee, F. B.: Mathematical Theory of Induced Voltage in the High-Tension Magneto. Scientific Paper, Bureau of Standards No. 424; 1922.

Reference 9. Silsbee, F. B.: Characteristics of High-Tension Magnetos. N. A. C. A. Technical Report No. 58; 1919.

Reference 10. Taylor-Jones, E.: Phil. Mag., 36, p. 145; 1918.

Reference 11. Silsbee, F. B.: Simplified Theory of the Magneto. N. A. C. A. Technical Report No. 123; 1921.

Reference 12. Silsbee, F. B.: Scientific Paper, Bureau of Standards No. 543; 1926.

NOTE

By F. B. SILSBEE

The most important part of the cycle of operation of an ignition system is that short interval between the instant at which the breaker opens the primary circuit and the time at which the spark occurs. It is the phenomena occurring during this short interval which determine the maximum value of the voltage which is attained and the speed with which this value is reached. These two values combined with the breakdown characteristics of the spark-plug gap completely determine whether or not a spark will occur. The electrical transients which take place during this interval in the circuits used in automotive ignition systems are so exceedingly rapid as to be beyond the effective range of the usual mechanical oscillographs.

The excellent mathematical analysis of Prof. E. Taylor-Jones gave a theoretical solution applicable when the circuits were free from shunting resistance, but the only direct experimental confirmation of his equations available prior to the work of Mr. Darnell consisted of (Reference 1) a few oscillograms taken by Professor Taylor-Jones with his ingenious electrostatic oscillograph on an induction coil which had considerably slower vibration periods than those common in ignition systems and a couple of voltage-time curves obtained at a great expense of labor and time by a point-by-point method developed by Paterson and Campbell. The development of the Dufour cathode-ray oscillograph in recent years has placed a far more powerful and convenient tool in the hands of the scientific investigator, and Mr. Darnell in the present work has used this tool with great patience and effectiveness to obtain a very brilliant confirmation of the predictions of Taylor-Jones's theoretical equations, in the range of conditions existing in commercial ignition coils. It is to be hoped that a similar study will be undertaken of the phenomena occurring in magnetos where the eddy current effects are usually of considerably greater importance.

The equations of Taylor-Jones apply directly to a circuit which the present writer has called a "two-coil model" of a spark generator. This model consists of two circuits magnetically coupled each containing resistance, inductance, and capacitance in series. As Darnell's results show, the frequencies computed for this model closely agree with those observed to exist, and there is every reason to expect a similar agreement in the induced voltages except to the extent that they are reduced by the effect of eddy currents which are not included in the 2-coil model. Unfortunately, however, this model does not cover the case in which there is a resistance in parallel with the secondary capacitance as is the case when a spark-plug insulator is fouled with a "carbon" deposit. Also the formulas deduced by Taylor-Jones for the induced secondary voltage are unavoidably so complicated that they are but little used by practical engineers.

In view of this situation the writer some years ago suggested (References 8, 11) other and simpler models which may be called the "single-coil model" and the "closed-coil model," which lead to rather simple final

equations for the secondary voltage developed under various conditions. It is the purpose of the present note to compare the values of voltage and frequency computed from these simpler equations with the experimental results of Mr. Darnell.

EFFECT OF PRIMARY CAPACITANCE

According to the single-coil model the primary and secondary capacitances, C_1 and C_2 respectively may be combined to give an effective capacitance which referred to the primary side is given by $C_1+n^2C_2$, when n is the mean turn ratio defined as $n=\sqrt{\frac{L_2}{L_1}}$. On this basis the frequency of the main oscillation is give by

$$f=\frac{1}{2\pi\sqrt{L_1(C_1+n^2C_2)}} \tag{1}$$

Values computed from equation (1) when compared with the data plotted in Figure 7 and Figure 10 of the paper are found to differ on the average by 3 per cent in the case of the Northeast coil and by 1 per cent in the case of the Delco coil. The greatest difference for any of the values taken was 6 per cent.

According to the single-coil model the crest voltage is given by

$$V_m=F\frac{I_b}{n}\sqrt{\frac{L_2}{C_1+n^2C_2}} \tag{2}$$

when I_b is the current at the instant of "break" and F is an empirical factor which allows for the effect of eddy currents and other losses in reducing the crest voltage below its ideal value. From the observed values of crest voltage plotted in Figure 8 the factor F can be computed for a number of values of C_1. It is found to range from 0.62 at the smallest value of C_1 to 0.78 at the largest, the mean value being 0.72. This small range $\pm$ 10 per cent in F indicates that the change of voltage by a factor of over 2 to 1 is fairly well represented by equation (2). The systematic increase in F with increase in C_1 can well be accounted for by the decrease in the damping effect of eddy currents with the decreasing frequency of the oscillations. Similar computations for the Delco coil show that in this case F ranges from 0.62 to 0.83 and has a mean value of 0.74. This mean value is in excellent agreement with the value 0.75 obtained on a similar coil by crest voltmeter measurements. (Reference 5.)

EFFECT OF SECONDARY CAPACITANCE

The same equations (1) and (2) should be expected to apply equally well to cases in which the secondary instead of the primary capacitance is varied. On comparing computed values of frequency with the observed values plotted in Figures 13 and 16 the average difference is found to be less than 1 per cent and in all but one case the individual differences were less than 5 per cent. The ratio F of observed to theoretical crest voltage is also fairly constant, the mean factors being 0.70 and 0.72 for the Northeast and Delco coils, respectively.

EFFECT OF A RESISTANCE IN PARALLEL WITH THE SECONDARY TERMINALS

When the insulator of a spark plug becomes coated with a conducting deposit of "carbon," the electrical system which most nearly approximates the actual conditions is that formed by two magnetically coupled circuits each containing resistance and inductance in series with capacitance, while in addition a resistance is connected in parallel with the secondary capacitance. The mathematical solution of the problem presented by the natural electrical oscillations in such a system while not perhaps impossible is certain to be so complicated as to come into little practical use. However, if the resistance which shunts the secondary terminals is considerably less than the reactance offered by the secondary capacitance, the latter would be expected to have but little effect on the oscillations and the system might be expected to behave in much the same way as would the "closed-coil model" which was suggested by the present writer in some earlier publications. (Reference 8.)

This closed-coil model consists of a primary circuit having in series the primary resistance, inductance, and capacitance of the ignition coil. This circuit is coupled magnetically by the normal coefficient of coupling of the coil windings to a secondary circuit which has in series the secondary inductance of the coil and the resistance of both the secondary winding and the shunting resistance. In such a model as the shunting resistance becomes lower the secondary crest voltage approaches the value given by the equation:

$$V=\frac{2I_bR_2}{n} \tag{3}$$

For the two coils tested the limiting value of V/R_2 from the observed data is 0.041 and 0.032 while the corresponding values of $2I_b/n$ are 0.048 and 0.035.

The computation of crest voltage for larger values of shunting resistance is rather laborious even with the simple closed-coil model. However, for the values of coupling coefficient met with in most ignition systems the curves given in Figure 20 of Scientific Paper No. 543 (Reference 12) enable the voltage to be computed quite easily.

In Figures 28 and 29 for the two coils, there are plotted on logarithmic paper in curves AB the crest voltage thus computed as ordinates against the shunting resistance as abscissas. Values of crest voltage read from Figures 20 and 22 of Darnell are plotted as crosses. It will be seen that the actual voltage is less than the theoretical by a fairly constant factor which for the Northeast coil is 0.68 and for the Delco coil is 0.81. These factors are not very different from those

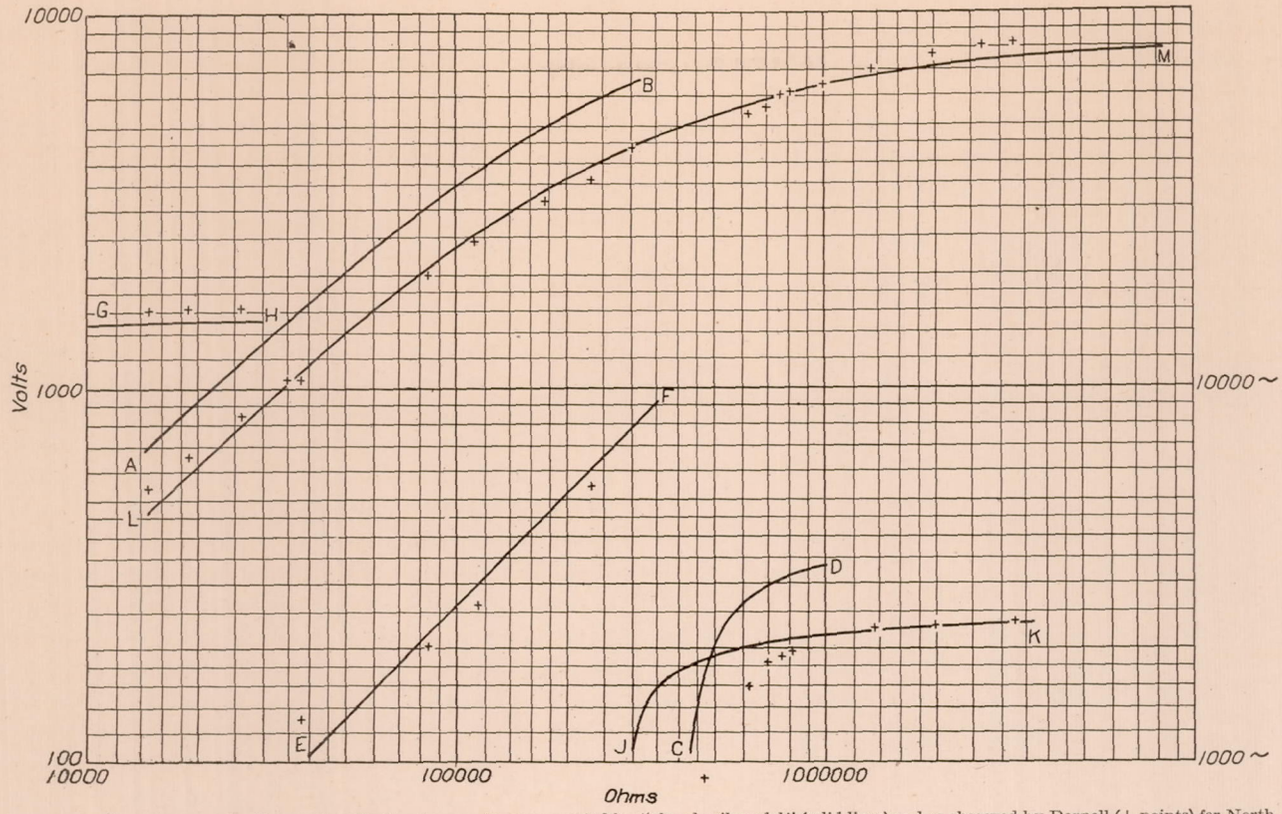

FIGURE 28.—Secondary crest voltage and oscillation frequencies as computed by "closed coil model" (solid lines) and as observed by Darnell (+ points) for Northeast coil

AB—Computed secondary crest voltage.
CD—Frequency as computed from equation (4).
EF—Computed damping exponent.
GH—Computed frequency for low values of R_2.
JK—Frequency as computed after allowing for secondary capacity.
LM—Secondary crest voltage computed from empirical equation (8).

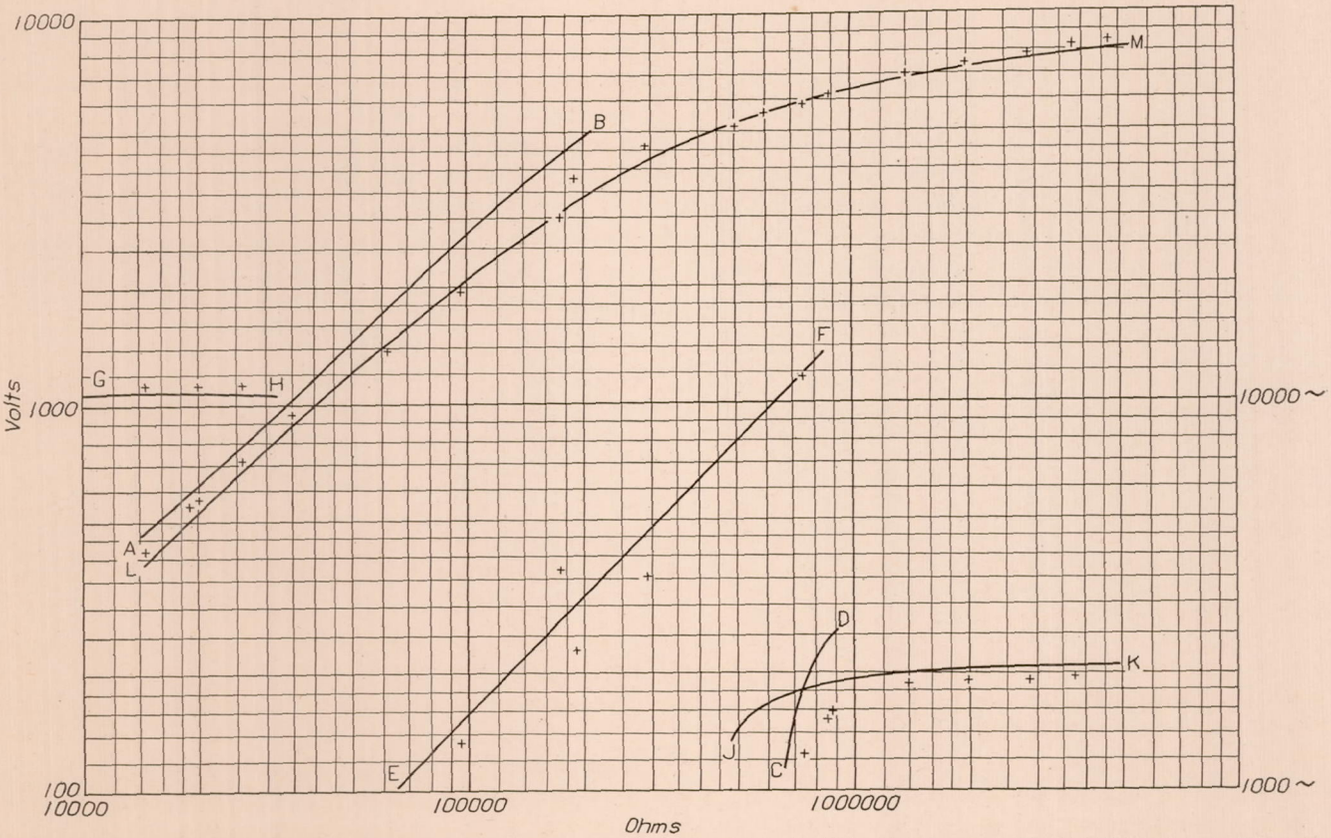

FIGURE 29.—Secondary crest voltage and oscillation frequencies as computed by "closed coil model" (solid lines) and as observed by Darnell (+ points) for Delco coil

AB—Computed secondary crest voltage.
CD—Frequency as computed from equation (4).
EF—Computed damping exponent.
GH—Computed frequency for low values of R_2.
JK—Frequency as computed after allowing for secondary capacity.
LM—Secondary crest voltage computed from empirical equation (8).

noted above in discussing the effect of adding capacitance and are doubtless attributable to the same eddy-current effects.

According to the closed-coil model the oscillations occurring when the shunting resistance, R_2, is fairly large, have a frequency given approximately by

$$f_1=\frac{1}{2\pi}\sqrt{\frac{1}{L_1C_1}-\frac{k^4L_2^2}{4R_2^2L_1^2C_1^2}} \tag{4}$$

As R_2 is decreased this frequency becomes less and the corresponding oscillation becomes more highly damped until at a particular value of R_2 given approximately by

$$R_2=\frac{k^2L_2}{2\sqrt{L_1C_1}} \tag{5}$$

the oscillation becomes aperiodic. Curves CD in Figures 28 and 29 give the frequencies computed from equation (4) for the respective coils.

For slightly lower values of R_2 the rate of subsidence of the impluse is governed largely by an exponential factor e^{m_1t} where m_1 is approximately equal to $\frac{-R_2}{L_2}\sqrt{L_1C_1}$. Lines EF in Figures 28 and 29 show the values of $^{-m}{}_1$ thus computed, the scale of $^{-m}{}_1$ in sec. $^{-1}$ being the same as that of frequency in cycles per second.

At still lower values of R_2 the closed-coil model predicts the existence of an oscillation of higher frequency superposed on the exponential transient, the frequency of which is plotted in curves GH.

On comparing these theoretical values with the observed results as given in Figure 19 of the original paper and as repeated in the plotted crosses in Figures 28 and 29, it appears that the high-frequency ripple observed at low values of shunting resistence has fairly closely the frequency predicted by the closed-coil model. At higher values of R_2, however, the secondary capacitance comes into play and this high-frequency ripple merges into the higher-frequency component which in turn is predicted by the 2-coil model for cases where the shunting effect of R_2 is absent.

The original photographic records permit of rough measurements of the exponential decay of the main transient for the cases when it is overdamped and the results of such measurements plotted as crosses show a fairly good agreement with the exponents computed theoretically (line EF).

The observed frequencies of the main component seem to trend toward zero at about the value of R_2 indicated by equation (5). At higher values of R_2, however, the observed frequencies are very markedly lower than the computed values plotted in curves CD. This is doubtless the result of the influence of the secondary capacitance which is not effectively short circuited at these high values of R_2. If the presence of this capacitance is allowed for by using the quantity $C_1+n^2C_2$ in place of C_1 in equation (4) the frequency values plotted in curve JK are obtained. These values are in excellent agreement with the observed frequencies at the higher values of shunting resistance but as would be expected, they depart very considerably at lower values of R_2.

In view of the difficulty of computing crest voltages even from the closed-coil model the writer has suggested the empirical equation

$$V=\frac{AR_2Z}{2R_2+Z} \tag{6}$$

connecting the crest voltage V and the shunting resistance R_2. If the constants A and Z are so chosen as to give values in agreement with those observed at $R_2=50{,}000$ ohms and 1,000,000 ohms the voltage for other resistances will be as indicated by the curves LM in Figures 28 and 29. It will be seen that the agreement between these curves and the observed values (plotted as crosses) is as close as is needed for practical work.

U. S. GOVERNMENT PRINTING OFFICE: 1931

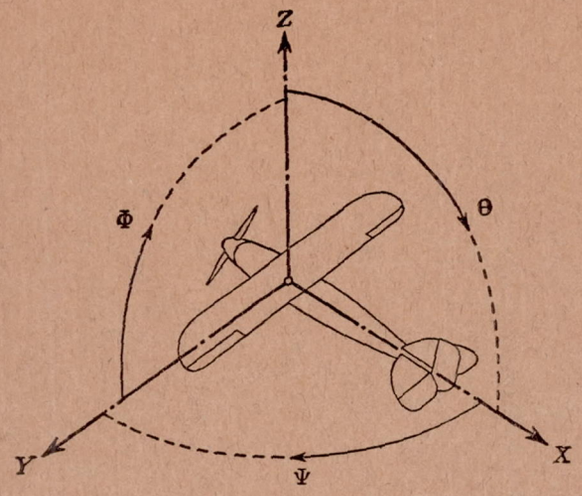

Positive directions of axes and angles (forces and moments) are shown by arrows

Axis		Force (parallel to axis) symbol	Moment about axis			Angle		Velocities	
Designation	Symbol		Designation	Symbol	Positive direction	Designation	Symbol	Linear (component along axis)	Angular
Longitudinal	X	X	rolling	L	$Y \longrightarrow Z$	roll	Φ	u	p
Lateral	Y	Y	pitching	M	$Z \longrightarrow X$	pitch	Θ	v	q
Normal	Z	Z	yawing	N	$X \longrightarrow Y$	yaw	Ψ	w	r

Absolute coefficients of moment

$$C_L = \frac{L}{qbS} \qquad C_M = \frac{M}{qcS} \qquad C_N = \frac{N}{qfS}$$

Angle of set of control surface (relative to neutral position), δ. (Indicate surface by proper subscript.)

4. PROPELLER SYMBOLS

D, Diameter.
p_e, Effective pitch.
p_g, Mean geometric pitch.
p_s, Standard pitch.
p_v, Zero thrust.
p_a, Zero torque.
p/D, Pitch ratio.
V', Inflow velocity.
V_s, Slip stream velocity.

T, Thrust.
Q, Torque.
P, Power.
(If "coefficients" are introduced all units used must be consistent.)
η, Efficiency $= T\ V/P$.
n, Revolutions per sec., r. p. s.
N, Revolutions per minute, r. p. m.
Φ, Effective helix angle $= \tan^{-1}\left(\frac{V}{2\pi rn}\right)$

5. NUMERICAL RELATIONS

1 hp = 76.04 kg/m/s = 550 lb./ft./sec.
1 kg/m/s = 0.01315 hp
1 mi./hr. = 0.44704 m/s
1 m/s = 2.23693 mi./hr.

1 lb. = 0.4535924277 kg
1 kg = 2.2046224 lb.
1 mi. = 1609.35 m = 5280 ft.
1 m = 3.2808333 ft.